

Original Article

Cite this article: Danukalova MK, Kuzmichev AB, Sennikov NV, and Tolmacheva TY (2020) Ordovician turbidites and black shales of Bennett Island (De Long Islands, Russian Arctic), and their significance for Arctic correlations and palaeogeography. *Geological Magazine* **157**: 1207–1237. <https://doi.org/10.1017/S0016756819001341>

Received: 23 January 2019
Revised: 7 October 2019
Accepted: 17 October 2019
First published online: 17 January 2020

Keywords:

New Siberian Islands; Siberia; graptolites; conodonts; early Palaeozoic; depositional environments; palaeoreconstructions

Author for correspondence:

Maria K. Danukalova,
Email: danukalovamk@yandex.ru

Ordovician turbidites and black shales of Bennett Island (De Long Islands, Russian Arctic), and their significance for Arctic correlations and palaeogeography

Maria K. Danukalova¹ , Alexander B. Kuzmichev¹, Nikolai V. Sennikov^{2,3} and Tatiana Yu. Tolmacheva⁴

¹Geological Institute, Russian Academy of Sciences, Pyzhevsky lane 7, Moscow, 119017, Russia; ²Trofimuk Institute of Petroleum Geology and Geophysics, Siberian Branch of the Russian Academy of Sciences, Koptug ave. 3, Novosibirsk, 630090, Russia; ³Novosibirsk State University, Pirogov St. 2, Novosibirsk, 630090, Russia and ⁴Karpinsky Russian Geological Research Institute, Sredny ave. 74, St. Petersburg, 199106, Russia

Abstract

Bennett Island stands alone in a remote part of the Arctic and information on its geology is essential to ascertain relations with other terranes in order to restore the early Palaeozoic Arctic palaeogeography. Lower Palaeozoic sedimentary rocks throughout the island were studied thoroughly for the first time. The Ordovician section (> 1.1 km thick) comprises three units: Tremadocian, lowest Floian black shale (130–140 m); Floian, lower Dapingian carbonate turbidite (> 250 m); and Dapingian, lower Darriwilian siliciclastic turbidite (> 730 m). Ordovician deposits conformably overlie Cambrian rocks deposited within the Siberian shelf, as shown earlier. Most of the Ordovician succession was formed in a deep trough that received carbonate debris from a nearby carbonate platform and silicate material from a distant landmass located to the NE (present coordinates). The Bennett Island Ordovician rocks have much in common with those of both the Central and Northern Taimyr belts. It could be tentatively suggested that both belts merged at their eastern continuation in the vicinity of De Long Islands. The whole system probably extends further eastwards. The Ordovician facies patterns and faunal assemblages in the New Siberian Islands are notably similar to those of northwestern Alaska, where the same lateral transition from turbidites to shelf limestones was reported.

1. Introduction

Bennett Island is located in the East Siberian Sea and belongs to the group of De Long Islands (the northern part of the New Siberian Islands archipelago, Fig. 1). The history of its discovery and study is associated with the names of the heroic pioneers George De Long, Eduard Toll and Alexander Kolchak, but the island remained poorly studied due to its remoteness. The first information on the geology of Bennett Island was reported by De Long's expedition, which discovered the island in 1881 (De Long, 1883). First geological samples were collected by EV Toll in 1902 (removed from the island in 1913; Toll, 1904). Almost all the documents disappeared along with his expedition. Later, short-term studies on the island were carried out in 1937 by MM Ermolaev and PA Shumsky (Ermolaev & Spizharsky, 1947). The only systematic study of the island's geology was carried out in 1956 by DA Vol'nov and DS Sorokov of the Arctic Geology Research Institute, St Petersburg, during the State geological mapping project of 1:1 000 000 scale (Vol'nov & Sorokov, 1961).

Bennett Island is composed of gently folded Cambrian and Ordovician marine rocks, unconformably overlain by Lower Cretaceous basalts. The Ordovician age of graptolitic shales collected by EV Toll was determined by G Troedssen (Ermolaev & Spizharsky, 1947). The Ordovician rocks were studied by MM Ermolaev and PA Shumsky, who described them as sandy shales and sandstones 500 m thick with rare calcareous varieties (Ermolaev & Spizharsky, 1947). During the State geological mapping project, the presence of Lower and Middle Ordovician rocks was confirmed by finds of Arenigian and lower Llandeilo graptolites (Vol'nov & Sorokov, 1961). Later publications indicated a narrower stratigraphic range of graptolite-bearing deposits corresponding to the late Arenigian–Llanvirn age, as a result of additional fossils collected by BA Klubov in 1972. The upper part of the section was conceivably attributed to the Llandeilo age (Vol'nov *et al.* 1970; Sobolevskaya, 1976). The Ordovician rocks were described by DA Vol'nov and DS Sorokov as a monotonous intercalation of siltstones, mudstones and sandstones of quartzose composition. It was mentioned that the amount of sandstones increases upwards, and that they show horizontal and cross-lamination as well as slump folds. In the visible top of the Ordovician strata, variegated sandstones were noted.

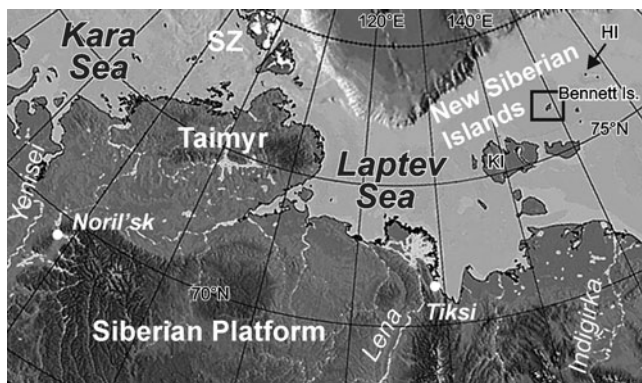


Fig. 1. Location of Bennett Island. HI – Henrietta Island; KI – Kotel'ny Island; SZ – Severnaya Zemlya.

The thickness of the Ordovician deposits was estimated as 1060–1080 m; the lower 300 m of the section does not crop out, and contact with the Cambrian rocks was not observed.

Sparse data on the Bennett Island Ordovician rocks resulted in different interpretations of their depositional and tectonic setting. The geology of the island differs from that of the southerly regions, and many researchers consider it as a part of an exotic (to Siberia) terrain (Şengör & Natal'in, 1996; Drachev, 2011). For example, SS Drachev (2011) interprets the lower Palaeozoic deposits of Bennett Island as distal turbidites, and suggests that the nearest outcrops of similar Cambrian and Ordovician rocks occur in northern Greenland, on Ellesmere Island, in the north of Alaska and in northern Yukon, NW Canada. According to the opposite point of view, first voiced by EV Toll, as well as the southerly islands of the archipelago, Bennett Island was part of the Siberian continent in the Palaeozoic (Toll, 1904; Cocks & Torsvik, 2011).

In June–September 2011, the first two authors conducted mapping and complex studies of the Bennett Island geology, in particular all the Ordovician exposures. This paper presents the results of studies on stratigraphy, fossils and sedimentology of the Ordovician sequence, along with conclusions on depositional environments and palaeogeography. A rich collection of graptolites was studied by NV Sennikov and conodonts were identified by TYu Tolmacheva.

In addition to the figures included in this article, there are a number of illustrations in online Supplementary Material 1 (available at <http://journals.cambridge.org/geo>), which are cited as Supplementary Figs S1–S32. We also provide colour versions of Figures 2, 3 and 4 in Supplementary Material 2.

2. General notes on the Ordovician sequence

The Ordovician rocks make up the eastern part of the island and are also exposed in the bottom of the northwestern coastal cliff (Fig. 2). The best outcrops are located on the western and northeastern coasts of the Chernyshev Peninsula and along the Pavel Keppen Bay (Fig. 3). The lowermost Ordovician beds crop out at the southern shore, near the mouth of the Four Crates River in the 273–277 points interval (Fig. 3), and in the banks of a nearby brook (points 278–281). The visible top of the section is exposed in a cliff 750 m NE from the mouth of the Lagernaya River (points 320, 321 and 102). An extensive inland area of Ordovician rocks in the eastern part of the island shown in

Figure 3 is mostly covered with a talus. Local rocky outcrops were found in the tributaries of the Lagernaya and the Four Crates rivers. Some Ordovician exposures were discovered for the first time.

The outcrops in the northwestern cliff are less extensive and more fragmented. Graptolite records showed that they do not overstep the stratigraphic interval of the eastern exposures. Nevertheless, they provided additional information to characterize the Ordovician rocks in terms of appearance, composition and sedimentology, allowing us to confirm the inclusion of all relevant information from the island, and enabling the general structure of the lower Palaeozoic deposits to be revealed.

Three units were recognized in the Ordovician section (from the bottom upwards; Fig. 4): black shale (130–140 m), carbonate turbidite (at least 250 m) and siliciclastic turbidite (at least 730 m). The total thickness of the Ordovician deposits is at least 1110 m. The variegated rocks described by DA Vol'nov and DS Sorokov (1961) at the top of the section have a secondary colouration, caused by (pre-?) Cretaceous weathering. They may occur at any stratigraphic level of the Palaeozoic deposits.

3. Black shale unit (Lower Unit of the Ordovician section): Tremadocian – lower Floian

The upper Cambrian and the lowermost Ordovician rocks on Bennett Island comprise a single succession of at least 250 m thickness, which is dominated by black shale. The name Dunbar Formation has been proposed for it (Danukalova *et al.* 2014). We refer to its upper portion as the Lower Unit of the Ordovician section. The exact position of the boundary between two systems could not be proven: the distance between the last point with the upper Cambrian trilobites (Aksai Stage, Danukalova *et al.* 2014) and the first occurrence of the Ordovician graptolites is about 600 m along the coast. This interval corresponds to c. 130 m of the true section's thickness (estimated geometrically). Most of it (90–100 m) we conditionally attribute to the Ordovician System, considering that the oldest graptolites (samples 275/1–275/3) indicate the Floian age; this barren interval must therefore include not only the uppermost Cambrian but the entire Tremadocian stages as well. We placed the boundary of the systems conditionally in the middle of an unexposed section along the shore between points 272 and 273 (Fig. 3). Judging by sparse outcrops, the barren part of the Ordovician section comprises loose black shale. In its middle part there is a package (≥ 15 m) containing beds of platy mudstone, including sandy varieties. Near the bottom of the package, a layer of brownish silty sandstone 30 cm thick has been found, while near the top of the package there is a limestone lens (25 × 100 cm). The overlying graptolite-bearing horizons of the unit are composed of grey and black, often rusty, foliated mudstone of c. 40 m thickness with inexplicit thin layers of sandy siltstones (Fig. 5), in which the Floian graptolites were found in three localities (the list of taxa from all the samples is given in Table 1). Graptolites in samples 275/1 and 275/2 (30 and 10 m below the top of black shale Unit, respectively) are characteristic for the middle and the upper parts of the Floian section. However, sample 275/3 in the top of the unit contains lower Floian graptolites. This fact, as well as the discovery of taxa typical of the basal Floian graptolite Zone *Tetragraptus approximatus* 10 m above the section forces us to limit (somewhat conventionally) the age of the Lower Unit as early Floian, or possibly the beginning of the middle Floian. Precise correlation between the boundary of the Lower and Middle units with the lower–middle Floian

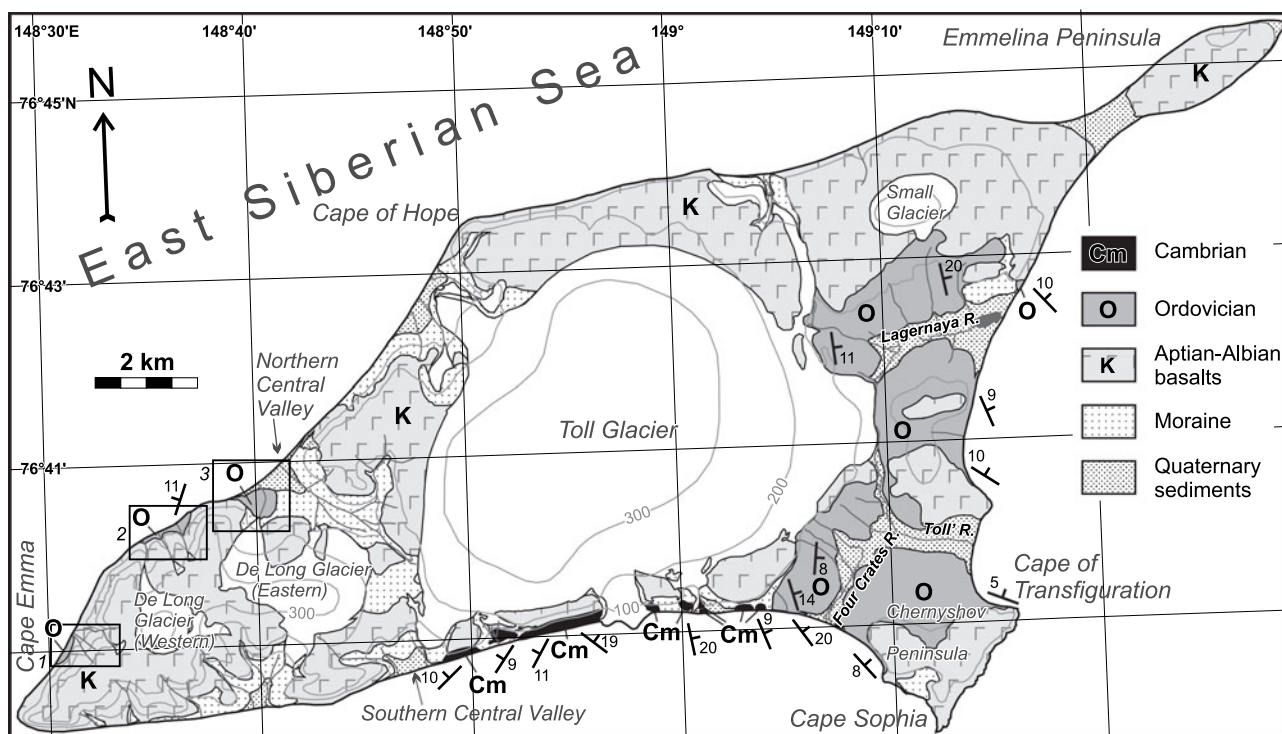


Fig. 2. Simplified geological map of Bennett Island, based on field observations. Black rectangles indicate the following areas within the western part of the island, where Ordovician outcrops were studied: 1, westernmost exposure; 2, Three Streams locality; 3, Northern Central Valley (see Sections 4 and 5).

boundary requires further study. According to our estimates, the total thickness of the Lower Ordovician black shale Unit is 130–140 m.

4. Carbonate turbidite unit (Middle Unit of the Ordovician section): lower Floian – lowest Dapingian?

The Middle Unit of the Ordovician section can be studied in rocky exposures in the following localities: to the west of the Four Crates River mouth (lower horizons that rest upon the black shale Unit, ‘1a’ and ‘1b’ in Fig. 6); to the SE of the mouth of this river in the cliff (outcrop 318–114, ‘2’ in Fig. 6); in a canyon of the lower right tributary of the Four Crates River (visible upper horizons of the Middle Unit in this part of the island, ‘3’ in Fig. 6), as well as on two localities in the NW of the island, Three Streams and Northern Central Valley (Fig. 2).

4.a. Lower horizons of the Middle Unit

The lowermost horizons of this Unit represent a continuation of the section mentioned above. In a low coastal outcrop 35 m to the west of point 276 and higher along the slope in the brook (point 279; Figs 3, 6), loose black shales of the Lower Unit are overlain by relatively solid mudstones and siltstones with layers of platy brownish-grey silty sandstone 0.5–1 cm thick (Supplementary Fig. S1). In a coastal outcrop this package contains rare thin layers of silty limestone. We attribute these rocks to the lowermost layers of the Middle Unit. Estimated geometrically, the thickness of the section’s fragment, exposed west of the Four Crates River mouth, does not exceed 30 m. Interbeds of limestone appear near the visible top in points 279–281, similar to those higher in the section. Graptolites characteristic of the *T. approximatus* Zone have been

found in the lower and in the upper parts of the fragment (samples 279/2 and 281/1).

4.b. Outcrop 318–114

The next outcrop is located to the east of the Four Crates River mouth, beginning at point 318 and heading SE to point 114 (Figs 3, 6). The estimated thickness of unexposed rocks around the river mouth is 75–85 m. The major part of this locality is a high cliff composed of the Ordovician rocks (up to 70 m) and crowned with Cretaceous basalt (Fig. 7). The lowermost horizons are exposed near point 318 at the beach and further in a low scarp, as well as at the SE end of the outcrop (point 114). The main part of the section is accessible only from sea ice. The visible top of the sequence was studied along the gully at 35–60 m above sea level (asl) by means of safety rope.

The lower 20–25 m of the sequence is composed of non-foliated solid mudstone with subtle layering and rare beds of limestone. The entire overlying part of the Middle Unit comprises carbonate flysch, a rhythmic alternation of dark grey mudstones and light grey limestones with a yellowish surface. A typical rhythm is shown in Figure 8. Some members of the rhythm may be absent. It can be seen in thin-sections that lower parts of the rhythms are composed of clastic rock, a carbonate siltstone or sandy siltstone (Supplementary Fig. S2). Apart from carbonate debris, silicate grains usually also occur, sometimes in considerable amounts (up to 40–50% in some layers). Those are mainly quartz with rare plagioclase and light mica. Semi-rounded grains predominate, but angular are also present. Mudstones can also contain silicate silt. In some thin-sections of siltstones, fragments of small shells of ostracods(?) have been found. Additionally, debris of chert was identified in siltstones; some lithic clasts resemble felsic lava.

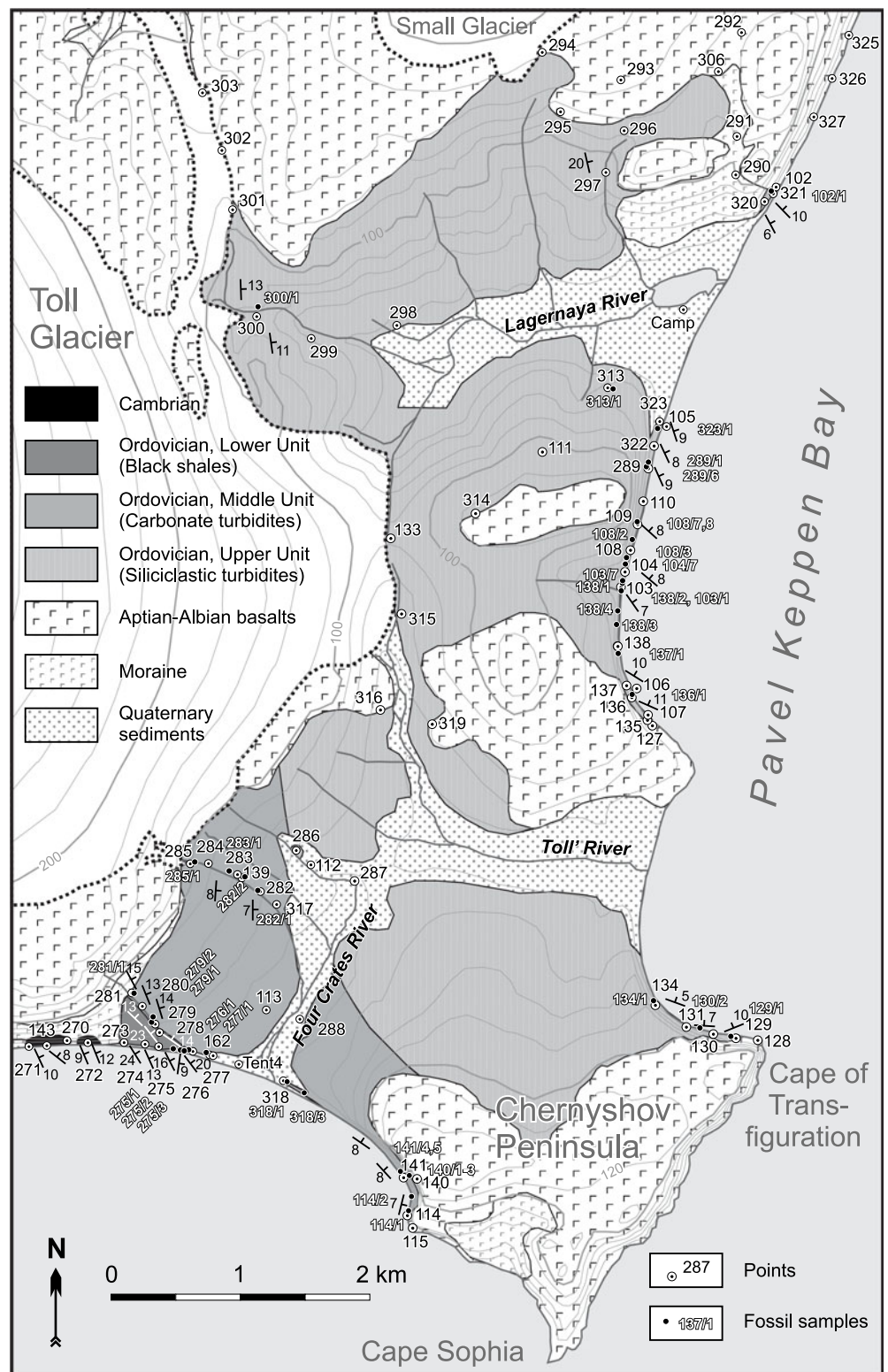


Fig. 3. Geological map of the eastern Bennett Island, where most of the Ordovician rocks crop out.

Carbonate layers often show sharp boundaries: both upper and lower (Fig. 9). At least in part, this is a result of the recrystallization and redistribution of carbonate matter to form concretion-like beds. Some limestone beds preserve cross-lamination and current ripple marks. The latter can be deformed by slumping. There are also rare amalgamation structures, convolute lamination and

furrows on the sole. About 30 m above the base of the described part of the section, a noticeable grey limestone bed (25–30 cm) with slump structures has been traced along the cliff (Fig. 9).

A glance at the cliff (Fig. 10) shows that the section comprises limestone-dominated and claystone-dominated alternating packages 1–3 m thick. From a distance, it is evident that the upper

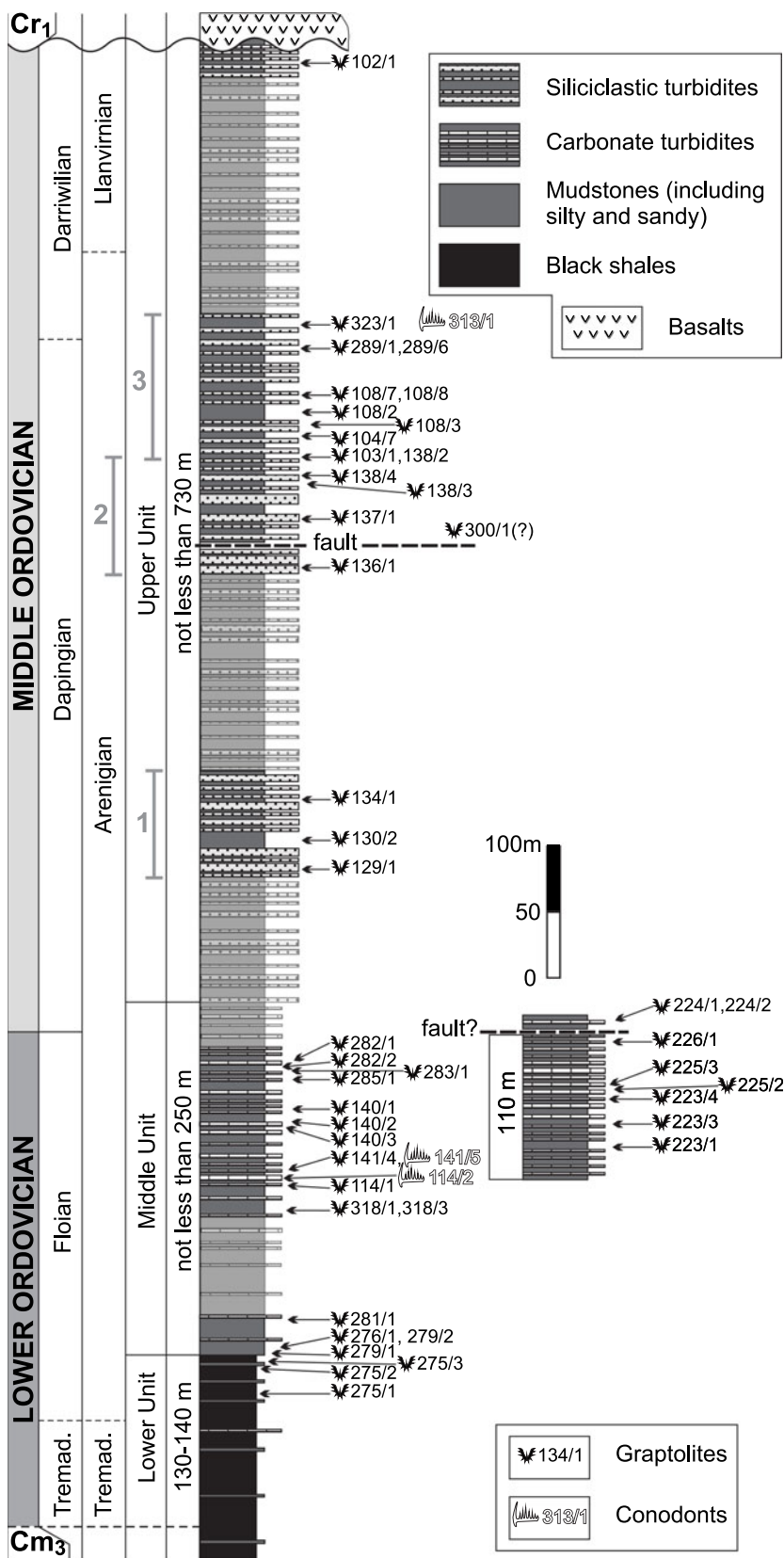


Fig. 4. Simplified stratigraphic column of the Ordovician deposits of Bennett Island. The main column represents sections studied in the eastern part of the island; the shorter column (right) represents the NW part (Three Streams locality). Lighter shading indicates parts of the section unexposed in cliff. Numbered bars to the left of column indicate intervals shown in more detail below in Figures 19, 22 and 24: 1, southern exposure; 2, key exposure, southern segment; 3, key exposure, northern segment; Cm₃ – Upper Cambrian; Cr₁ – Lower Cretaceous; Tremad. – Tremadocian.

part of the cliff differs from grey-coloured carbonaceous flysch common to the Unit and is composed of contrasting packs of yellow and brown rocks, intercalating with dark grey and black horizons. With the help of a safety rope, it was confirmed that

the upper part of the visible section contains no new lithologies or sedimentary structures. The unusual appearance and high contrast between limestones and shales were caused by pre-Cretaceous weathering.



Fig. 5. (Colour online) Foliated mudstones with thin siltstone beds. Upper part of the Black shale Unit, Lower Floian.

The total thickness of the exposed rocks in outcrop 318–114 is 110 m, estimated from the photograph panoramas including a range pole.

A rich complex of Floian graptolites was found (sample 318/1) in the base of the section visible in this outcrop near point 318. Graptolites of the *T. approximatus* Zone of the lower Floian Stage (sample 318/3) were revealed in the deposits several metres up section. Sample 114/1 revealed Early and Middle Ordovician graptolites, mostly poorly preserved, at 26–28 m above the base. These included *Phyllograptus densus* Tornquist, which is nominal for the same name Zone of the middle Floian Stage. A few metres higher, the marking layer of limestone (the layer with slump folds mentioned above) yielded conodonts (sample 114/2; Table 1) of late Floian age (bottom of the *Oepikodus evae* Zone). A similar complex of conodonts (sample 141/5) was found *c.* 4 m above, as well as a few Early–Middle Ordovician graptolites (sample 141/4; Fig. 10). In the upper part of the section (approximately 28.5 and 38 m below the visible top of the Unit, samples 140/1 and 140/2, respectively), weathered rocks contain graptolites that can be identified only up to the genus; all of these are transit forms of Early–Middle Ordovician age. Unexpectedly, a complex of graptolites (sample 140/3) containing the form *Expansograptus hirundo* (Salter) was found 42.5 m below the visible top of the Unit. The presence of this species indicates that the rocks belong to the eponymous zone of the upper Dapingian strata, and additional study of the palaeontological material is required.

4.c. Subglacial Canyon in the Four Crates River valley

Another exposure of the carbonate turbidite Unit was found 1.5 km NNW from the mouth of the Four Crates River, in the upper course of its largest right tributary (Figs 3, 6). A stream flowing from under the Toll glacier has cut a canyon 2–4 m deep; the Ordovician rocks crop out in the steep walls of this canyon, accessible only at the end of summer when the glacier melt is not so active. During the first half of summer, the stream is a turbulent current with huge rolling blocks flowing in a tunnel under a thick snowdrift. The canyon originally formed under the Toll glacier, which has now retreated up the slope.

The rocks exposed here augment that of outcrop 318–114. The stream flows across the strike of the rocks, but the channel slope is very close to the dip angle (7–8°) so the true thickness of the exposed rocks is only 15–20 m. Primary sedimentary structures are well preserved in this outcrop and clearly visible in canyon walls. The creek goes under permanent ice near point 284, and further upstream only bedrock talus and rare outcrops are observed. The last Palaeozoic outcrop was described at point 285, where the rocks are tinted in the weathering crust. Downcurrent between points 282 and 317, the Ordovician bedrocks only crop out episodically.

This part of the Middle Unit is formed of grey with ochre surface, non-laminated and cross-laminated fine-grained limestones and clayey limestones, alternating with comparatively solid darker mudstone (Supplementary Fig. S3). The carbonate layers range in thickness from a few millimetres to 20 cm. The layers are concretion-like in places and sometimes exhibit convolute lamination (Fig. 11a) and current ripples in places. Some intricate structures are interpreted as deformed current ripples, submerged in the underlying mud and covered by silt with undisturbed planar lamination (Fig. 11b). Current direction may not have been uniform; in some cases current ripples show opposite dips in different beds. In addition, some limestone layers in the canyon demonstrate gently undulating cross-stratification (Fig. 11c, Supplementary Fig. S4). This feature, which resembles hummocky cross-stratification (HCS), is known for some turbidite assemblages (see Section 4.e).

Graptolites have been found at four sites within the canyon. Three samples (282/1, 282/2 and 283/1) contain the species *Didymograptus protobifidus* Elles, nominal of the eponymous Zone of late Floian time. At the lower point (sample 285/1), the poorly preserved recovered graptolites are of Early–Middle Ordovician age.

4.d. Carbonate turbidite unit in the NW of the island

4.d.1. Three Streams locality

A considerable and impressive fragment of the Ordovician section is exposed (Figs 12, 13) in the cliff of the NW coast of Bennett Island, northwards of the western De Long glacial dome (Fig. 2).

Table 1. Graptolite and conodont (highlighted) faunas from Ordovician rocks on Bennett Island. Location of the samples and their position on columns are shown in Figures 3, 4, 10, 12, 17, 20, 23, 26 and 29. The relative stratigraphic position of samples 170/1, 170/2, 171/2, 171/3, 172/1 and 259/1 (see Fig. 17) in the sequence is undetermined, but all belong to a single interval several tens of metres thick.

Sample no.	Taxa present	Age	Zone
Black shale Unit			
275/1	<i>Expansograptus</i> cf. <i>suecicus</i> (Tullberg), <i>Expansograptus</i> cf. <i>extensus</i> (Hall), <i>Acrograptus cognatus</i> (Harris et Thomas), <i>Pseudisograptus</i> sp., <i>Isograptus</i> sp.	Floian–Dapingian	
275/2	<i>Eotetragraptus harti</i> (TS Hall), <i>Expansograptus</i> sp.	Floian–Dapingian	
275/3	<i>Eotetragraptus aequalis</i> Tzaj, <i>Eotetragraptus quadribrachiatus</i> (Hall), <i>Eotetragraptus harti</i> (TS Hall), <i>Expansograptus</i> sp., <i>Goniograptus</i> sp.	Early Floian	
Carbonate turbidite Unit (south Bennett Island)			
279/1	<i>Eotetragraptus aequalis</i> Tzaj, <i>Eotetragraptus</i> cf. <i>quadribrachiatus</i> (Hall)	Early Floian	
279/1a	<i>Eotetragraptus quadribrachiatus</i> (Hall), <i>Eotetragraptus aequalis</i> Tzaj, <i>Eotetragraptus</i> sp.	Early Floian	
279/2	<i>Paratetragraptus approximatus</i> (Nicholson), <i>Paratetragraptus acclinans</i> (Keble), <i>Eotetragraptus</i> cf. <i>quadribrachiatus</i> (Hall), <i>Eotetragraptus aequalis</i> Tzaj, <i>Eotetragraptus</i> sp., <i>Pseudisograptus</i> sp., <i>Expansograptus</i> sp.	Early Floian	<i>T. approximatus</i>
276/1	<i>Expansograptus similis</i> (Hall), <i>Expansograptus</i> cf. <i>latus</i> (Hall), <i>Expansograptus</i> sp., <i>Phyllograptus</i> sp.	Floian	
281/1	<i>Paratetragraptus approximatus</i> (Nicholson), <i>Paratetragraptus</i> aff. <i>acclinans</i> (Keble), <i>Eotetragraptus quadribrachiatus</i> (Hall), <i>Isograptus</i> sp.	Early Floian	<i>T. approximatus</i>
318/1	<i>Eotetragraptus harti</i> (TS Hall), <i>Eotetragraptus aequalis</i> Tzaj, <i>Eotetragraptus quadribrachiatus</i> (Hall), <i>Paratetragraptus approximatus</i> (Nicholson), <i>Paratetragraptus</i> ex gr. <i>approximatus</i> (Nicholson), <i>Pseudodichograptus</i> sp., <i>Brachiograptus</i> sp., <i>Pendograptus</i> sp., <i>Phyllograptus</i> sp., <i>Acrograptus cognatus</i> (Harris et Thomas), <i>Acrograptus nicholsoni</i> (Lapworth), <i>Expansograptus suecicus</i> (Tullberg)	Floian	
318/3	<i>Paratetragraptus approximatus</i> (Nicholson), <i>Eotetragraptus harti</i> (TS Hall), <i>Expansograptus latus</i> (Hall), <i>Dichograptus</i> sp.	Early Floian	<i>T. approximatus</i>
114/1	<i>Phyllograptus densus</i> Tornquist, <i>Phyllograptus</i> cf. <i>anna</i> Hall, <i>Phyllograptus</i> sp., <i>Expansograptus suecicus</i> (Tullberg), <i>Expansograptus</i> cf. <i>latus</i> (T.S. Hall), <i>Expansograptus</i> cf. <i>extensus</i> (Hall), <i>Expansograptus</i> sp., <i>Eotetragraptus harti</i> (TS Hall), <i>Eotetragraptus</i> sp., <i>Paratetragraptus</i> sp., <i>Dichograptus</i> sp.	Middle Floian	<i>P. densus</i>
114/2 (conodonts)	<i>Oepikodus</i> cf. <i>intermedius</i> (Serpagli), <i>Protoprioniodus papillosus</i> (van Wamel), <i>Paracordylodus gracilis</i> Lindström, <i>Kallidontus corbatoi</i> (Serpagli), <i>Cornuodus longobasis</i> (Lindstrom), <i>Acodus</i> sp., <i>Drepanodus</i> sp.	Late Floian	<i>O. evae</i> (lowermost part)
141/4	<i>Expansograptus suecicus suecicus</i> (Tullberg), <i>Isograptus</i> sp., <i>Didymograptus</i> cf. <i>indentus</i> (Hall)	Early–Middle Ordovician	
141/5 (conodonts)	<i>Oepikodus</i> cf. <i>intermedius</i> (Serpagli), <i>Protoprioniodus papillosus</i> (van Wamel), <i>Paracordylodus gracilis</i> Lindström, <i>Kallidontus corbatoi</i> (Serpagli), <i>Cornuodus longobasis</i> (Lindstrom), <i>Acodus</i> sp., <i>Drepanodus</i> sp.	Late Floian	<i>O. evae</i> (lowermost part)
140/3	<i>Expansograptus hirundo</i> (Salter), <i>Tetragraptus bigsbyi latus</i> Hsu, <i>Tetragraptus</i> (?) sp., <i>Isograptus paraboloides</i> Tzaj, <i>Phyllograptus</i> sp.	Late Dapingian	<i>E. hirundo</i>
140/2	<i>Didymograptus</i> sp., <i>Expansograptus</i> sp.	Early–Middle Ordovician	
140/1	<i>Tetragraptus</i> ex gr. <i>bigsbyi</i> (Hall), <i>Didymograptus</i> aff. <i>protobifidus</i> Elles, <i>Didymograptus</i> aff. <i>stabilis</i> Elles et Wood, <i>Didymograptus</i> ex gr. <i>indentus</i> (Hall), <i>Didymograptus</i> sp., <i>Isograptus</i> sp., <i>Phyllograptus</i> sp., <i>Pseudophyllograptus angustifolius elongatus</i> Bulman	Early–Middle Ordovician	
285/1	<i>Tetragraptus</i> (?) sp., <i>Didymograptus</i> sp.	Early–Middle Ordovician	
283/1	<i>Didymograptus protobifidus</i> Elles, <i>Tetragraptus bigsbyi</i> (Hall), <i>Expansograptus</i> sp., <i>Phyllograptus</i> sp.	Late Floian	<i>D. protobifidus</i>
282/2	<i>Eotetragraptus harti</i> (TS Hall), <i>Didymograptus protobifidus</i> Elles, <i>Expansograptus</i> sp.	Late Floian	<i>D. protobifidus</i>
282/1	<i>Didymograptus protobifidus</i> Elles, <i>Isograptus</i> sp.	Late Floian	<i>D. protobifidus</i>

(Continued)

Table 1. (Continued)

Sample no.	Taxa present	Age	Zone
Carbonate turbidite Unit (NW Bennett Island)			
170/2	<i>Eotetraraptus harti</i> (TS Hall), <i>E. sp.</i> , <i>Expansograptus sp.</i>	Floian–Dapingian	
171/2	<i>Paratetraraptus acclinans</i> (Keble), <i>P. akzharensis</i> Tzaj	Early Floian	<i>T. approximatus</i>
171/3	<i>Pendeograptus pendens</i> (Elles), <i>Paratetraraptus approximatus</i> (Nicholson)	Early Floian	<i>T. approximatus</i>
172/1	<i>Eotetraraptus harti</i> (TS Hall), <i>Tetraraptus bigsbyi</i> (Hall)	Floian–Dapingian	
259/1	<i>Paratetraraptus approximatus</i> (Nicholson), <i>Paratetraraptus sp.</i> , <i>Eotetraraptus sp.</i> , <i>Clonograptus sp.</i>	Early Floian	<i>T. approximatus</i>
223/1	<i>Didymograptus protobifidus</i> Elles, <i>Pendeograptus aff. fruticosus</i> (Hall), <i>Clonograptus sp.</i> , <i>Tetraraptus (?) sp.</i> , <i>Isograptus sp.</i> , <i>Expansograptus extensus</i> (Hall)	Late Floian	<i>D. protobifidus</i>
223/3	<i>Isograptus sp.</i> , <i>Didymograptus protobifidus</i> Elles, <i>Pendeograptus sp.</i>	Early–Middle Ordovician	
223/4	<i>Phyllograptus typus</i> Hall, <i>Phyllograptus sp.</i> , <i>Oncograptus cf. upsilon</i> TS Hall, <i>Didymograptus eobifidus</i> Chen et Xia	Floian	
225/2	<i>Didymograptus protobifidus</i> Elles, <i>Didymograptus sp.</i> , <i>Expansograptus suecicus</i> (Tullberg), <i>Tetraraptus sp.</i> , <i>Paratetraraptus sp.</i> (determination is performed from field photographs)	Floian	
225/3	<i>Eotetraraptus sp.</i> , <i>Didymograptus cf. indentus</i> (Hall), <i>Didymograptus cf. acutus</i> Ekstrom, <i>Isograptus hemicyclus</i> (Harris), <i>Expansograptus extensus</i> (Hall)	Early–Middle Ordovician	
226/1	<i>Zygograptus sp.</i> , <i>Tetraraptus sp.</i> , <i>?Paratetraraptus sp.</i> , <i>Phyllograptus cf. anna</i> Hall, <i>Phyllograptus rotundatus</i> Mosen, <i>Phyllograptus sp.</i> , <i>Expansograptus sp.</i> , <i>Didymograptus sp.</i> (determination is performed from field photographs)	Floian	
224/1	<i>Corymbograptus deflexus</i> (Elles et Wood). Additional determination from field photographs: <i>Expansograptus latus</i> (Hall), <i>Expansograptus taimyrensis</i> Obut et Sobolevskaya, <i>Expansograptus sp.</i> , <i>Corymbograptus sp.</i> , <i>Isograptus sp.</i> , <i>Tetraraptus sp.</i> , <i>Eotetraraptus sp.</i>	Early Dapingian	<i>I. gibberulus</i> , <i>C. deflexus</i> Subzone
224/2	<i>Corymbograptus v-fragosus</i> Obut et Sobolevskaya, <i>Expansograptus latus</i> (TS Hall), <i>Didymograptus cf. indentus</i> (Hall)	Middle Ordovician	
Siliciclastic turbidite Unit (exposures in Pavel Keppen Bay)			
129/1	<i>Phyllograptus sp.</i> , <i>Isograptus paraboloides</i> Tzaj, <i>Isograptus sp.</i> , <i>Expansograptus sp.</i>	Early Dapingian	<i>I. gibberulus(?)</i>
130/2	<i>Tetraraptus(?) sp.</i> , <i>Phyllograptus sp.</i> , <i>Tristichograptus sp.</i> , <i>Isograptus paraboloides</i> Tzaj, <i>Isograptus caduceus</i> (Salter)	Dapingian	
130/2a	<i>Isograptus caduceus</i> (Salter), <i>Isograptus sp.</i>	Dapingian	
134/1	<i>Paratetraraptus sp.</i> , <i>Eotetraraptus sp.</i> , <i>Tetraraptus sp.</i> , <i>Isograptus sp.</i>	Early–Middle Ordovician	
136/1	<i>Isograptus caduceus nanus</i> (Ruedemann), <i>Zygograptus sp.</i> , <i>?Undulograptus–Glyptograptus sp.</i> , <i>Tetraraptus(?) sp.</i> , <i>Loganograptus logani</i> (Hall)	Dapingian	
137/1	<i>Isograptus maximo-divergens</i> (Harris), <i>Expansograptus sp.</i> , <i>Tetraraptus bigsbyi</i> (Hall), <i>Paraglossograptus sp.</i> , <i>Glyptograptus sp.</i>	Early Dapingian	<i>I. gibberulus</i> , <i>I. maximo-divergens</i> Subzone
138/3	<i>Isograptus gibberulus</i> (Nicholson), <i>Clonograptus sp.</i> , <i>Glossograptus sp.</i>	Early Dapingian	<i>I. gibberulus</i>
138/4	<i>Tristichograptus augustus</i> Mu et Lee	Early–Middle Ordovician	
138/2	<i>Tetraraptus(?) sp.</i> , <i>Tristichograptus ensiformis</i> (Hall), <i>Isograptus gibberulus</i> (Nicholson), <i>Isograptus sp.</i> , <i>Pseudodichograptus sp.</i> , <i>Glossograptus sp.</i> , <i>Paraglossograptus sp.</i> , <i>Glyptograptus sp.</i>	Early Dapingian	<i>I. gibberulus</i>
103/1	Transitional forms <i>Undulograptus cf. sinodontatus</i> (Mu et Lee) – <i>Undulograptus cf. austrodonatus</i> (Harris et Keble), <i>Undulograptus sp.</i> , <i>Expansograptus sp.</i> , <i>Acrograptus sp.</i> , <i>Isograptus sp.</i> , <i>Glossograptus(?) sp.</i>	Dapingian – early Darriwilian	
103/7	<i>Loganograptus logani</i> (Hall), <i>Cryptograptus sp.</i> , <i>Pendeograptus sp.</i> , <i>Eotetraraptus sp.</i>	Early–Middle Ordovician	
138/1	<i>Glossograptus hincksi</i> (Hopkinson), <i>Tetraraptus(?) sp.</i> , <i>Tristichograptus sp.</i> , <i>Isograptus ex gr. maximo-divergens</i> (Harris), <i>Isograptus sp.</i> , <i>Paraglossograptus sp.</i>	Early Dapingian	<i>I. gibberulus</i> , <i>I. maximo-divergens(?)</i> Subzone

(Continued)

Table 1. (Continued)

Sample no.	Taxa present	Age	Zone
104/7	<i>Isograptus gibberulus</i> (Nicholson)	Early Dapingian	<i>I. gibberulus</i>
108/3	<i>Glossograptus</i> sp., <i>Cryptograptus</i> sp.	Early–Middle Ordovician	
108/2	<i>Phyllograptus</i> sp.	Early–Middle Ordovician	
108/7	<i>Tristichograptus ensiformis</i> (Hall), <i>Loganograptus logani</i> (Hall), <i>Loganograptus</i> sp., <i>Pseudotrigraptus</i> sp., <i>Tetragraptus</i> (?) sp., <i>Isograptus caduceus nanus</i> Ruedemann, <i>Expansograptus</i> sp., <i>Glyptograptus</i> sp., <i>Acrograptus</i> sp., <i>Cryptograptus</i> sp., <i>Paraglossograptus</i> sp., <i>Glossograptus acanthus</i> Elles et Wood	Late Dapingian	<i>E. hirundo</i>
108/8	<i>Tetragraptus bigsbyi</i> (Hall), <i>Eotetragraptus harti</i> (TS Hall), <i>Eotetragraptus</i> ex gr. <i>quadribrachiatus</i> (Hall), <i>Eotetragraptus</i> sp., <i>Loganograptus</i> sp., <i>Isograptus shrenki</i> Obut et Sobolevskaya, <i>Glossograptus acanthus</i> Elles et Wood	Dapingian – early Darriwilian	
289/6	<i>Glossograptus acanthus</i> Elles et Wood, <i>Expansograptus</i> sp., <i>Tetragraptus</i> (?) sp., <i>Phyllograptus</i> sp., <i>Cryptograptus</i> sp., <i>Corymbograptus</i> cf. <i>deflexus</i> (Elles et Wood), <i>Tristichograptus</i> sp., <i>Didymograptus</i> sp.	Dapingian – early Darriwilian	
289/1	<i>Isograptus</i> sp., <i>Acrograptus</i> sp., <i>Tristichograptus</i> sp., <i>Glyptograptus</i> sp.	Early–Middle Ordovician	
323/1	<i>Tetragraptus bigsbyi</i> (Hall), <i>Eotetragraptus harti</i> (TS Hall), <i>Tristichograptus augustus</i> Mu et Lee, <i>Tristichograptus</i> sp., <i>Pendeograptus pendus</i> (Elles), <i>Bryograptus</i> sp., <i>Phyllograptus</i> sp., <i>Acrograptus cognatus</i> (Harris et Thomas), <i>A.</i> sp., <i>Isograptus gibberulus</i> (Nicholson), <i>Isograptus</i> cf. <i>forcipiformis</i> (Ruedemann), <i>Isograptus reduncus</i> Tzaj, <i>Isograptus caduceus nanus</i> Ruedemann, <i>Tetragraptus</i> (?) sp., <i>Didymograptus</i> cf. <i>indentus</i> (Hall), <i>Expansograptus</i> sp., <i>Cryptograptus</i> sp., <i>Glossograptus</i> sp.	Dapingian – early Darriwilian	<i>E. hirundo</i> (?)
102/1	<i>Paratetragraptus</i> sp., <i>Tristichograptus</i> sp., <i>Acrograptus</i> sp., <i>Pseudophyllograptus angustifolius tenuis</i> (Monsen), <i>Pseudophyllograptus angustifolius elongatus</i> Bulman, <i>Phyllograptus ilicifolius</i> Hall, <i>Phyllograptus</i> sp., <i>Corymbograptus</i> cf. <i>deflexus</i> (Elles et Wood), <i>Expansograptus suecicus</i> (Tullberg), <i>E.</i> sp., <i>Isograptus</i> cf. <i>forcipifonus</i> (Ruedemann), <i>Isograptus hemicyclus</i> (Harris), <i>Pseudobryograptus</i> sp., <i>Hollograptus</i> sp., <i>Goniograptus</i> sp., <i>Glyptograptus</i> sp., <i>Cryptograptus</i> sp., <i>Glossograptus</i> sp., <i>Paraglossograptus</i> sp., <i>Brachiograptus</i> sp.	Dapingian – early Darriwilian	
Siliciclastic turbidite Unit (local exposures in Lagernaya River valley)			
300/1	<i>Isograptus gibberulus</i> (Nicholson), <i>Isograptus paraboloides</i> Tzaj, <i>Isograptus</i> sp., <i>Tetragraptus</i> (?) sp., <i>Eotetragraptus</i> sp., <i>Expansograptus suecicus</i> (Tullberg), <i>Phyllograptus</i> sp., <i>Loganograptus</i> sp., <i>Dichograptus</i> sp., <i>Pendeograptus</i> sp.	Early Dapingian	<i>I. gibberulus</i>
313/1 (conodonts)	<i>Paroistodus horridus</i> (Barnes et Poplawski), <i>Periodon macrodentata</i> (Graves et Ellison), <i>Spinodus spinatus</i> (Hadding), <i>Polonodus</i> sp., <i>Ansella</i> sp., <i>Scolopodus</i> sp., <i>Acodus</i> sp., <i>Costiconus</i> sp.	Early Darriwilian	
Siliciclastic turbidite Unit (NW Bennett Island)			
249/1	<i>Isograptus gibberulus</i> (Nicholson), <i>Isograptus maximo-divergens</i> (Harris), <i>Isograptus</i> sp., <i>Expansograptus extensus</i> (Hall), <i>Phyllograptus typus</i> Hall, <i>Corymbograptus deflexus</i> (Elles et Wood)	Early Dapingian	<i>I. gibberulus</i> , <i>I. maximo-divergens</i> Subzone

This location is difficult to access in the absence of fast ice. The three deep gullies, from which this area was named, run approximately from the south to the north. In our attempts to get from the basalt plateau to the shoreline we tried all of them. However, they were narrow, steep and deeply cut gorges, filled in the upper parts with snowfields or, in the case of the westernmost gully, the tongue of the De Long glacier. Two of the gullies ended with waterfalls at an altitude of 50–70 m asl. The descent is possible only along the eastern valley, which is well developed and ends with a 10 m steep drop, covered by a permanent snowfield.

The cliffs comprise Ordovician rocks from their lower part up to an altitude of 50–80 m, and stretch for 1.2 km along the shore. In the eastern part of the outcrop, near the contact with the Cretaceous deposits, the Ordovician rocks are coloured in the

weathering crust and dislocated; some intervals are covered with scree. The Ordovician section is continuous to the west; a thick scree covers it only between points 225 and 226. The beach is passable over the entire length of the Ordovician outcrop. The rocks comprise a homocline, dipping by 6–11° towards the W-WNW. The sequence is displaced by several normal faults of low amplitude near point 225, as well as over an interval of 210 m from point 223 westwards. The total thickness of the exposed section is not less than 110 m (estimated geometrically, eastern part not included).

The carbonate flysch at the Three Streams locality appears with more contrast than at the southern coast of the island, and sedimentary structures are better preserved (Fig. 14). In general, the lower half of the section demonstrates fine alternation with beds thicknesses from 2 to 10 cm, rarely larger (Supplementary Fig. S5A). Higher in the section, the alternation becomes more

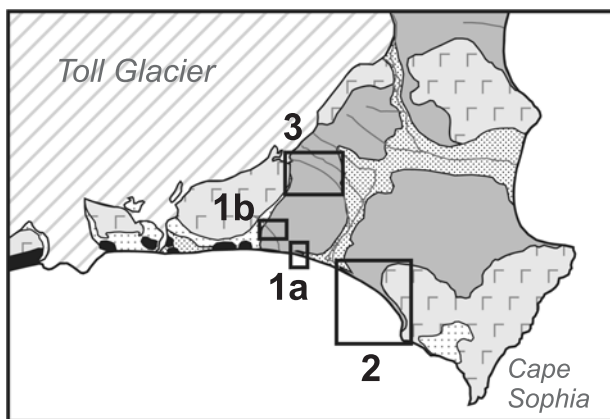


Fig. 6. Location of the Middle Unit outcrops in the eastern part of Bennett Island: 1, lower part of the Unit (1a, in a low cliff; 1b, in a stream on the hillside); 2, outcrop 318–114 (Four Crates); 3, subglacial Canyon. Uniform grey shading corresponds to the Ordovician rocks. Black shading highlights the location of Cambrian rocks.

coarse with a predominance of clastic limestone of thickness 10–20 cm and more (Supplementary Fig. S5B). Near the visible top of the section, the thickness of the beds decreases again. Light-coloured rocks in the section are carbonate siltstones and fine-grained carbonate sandstones. The layers are generally of constant thickness, but some show pinches and bulges (Supplementary Fig. S5A, left side). Different variants of geometry have been observed. One type of such beds have a flat sole and undulating top, resembling the HCS shape, with a distance between hummocks of c. 0.5–1.0 m (Supplementary Fig. S6). More often, both the roof and the sole of beds are wavy, giving the appearance of a chain of connected lenses (Supplementary Fig. S7). One type can pass into another along the strike. The carbonate rocks demonstrate planar and gently undulating lamination (Supplementary Fig. S8), cross-stratification, convolute bedding (Fig. 15a), current ripples (Supplementary Fig. S8B) and, rarely, climbing ripples (Fig. 15b). All structures listed above often show soft-sediment deformations, as in Section 4.c (Supplementary Fig. S9). Some layers contain barely identifiable irregular load marks and flute casts. Normal-graded beds occur. The darker elements of the section are mudstones (usually calcareous) with a conchoidal fracture, as well as low-carbonate siltstones, sometimes containing fragments of disrupted layers of carbonate sandstone (Fig. 15c).

The Ordovician deposits studied in the Three Streams section apparently correspond to the upper part of the carbonate turbidite Unit. The Floian graptolites (samples 223/1, 223/4, 225/2, 226/1) were found in its different levels; notably, the series of samples 223/1 collected at the bottom of the sequence contains the species *Didymograptus protobifidus* Elles, nominal for the eponymous Zone of late Floian age. This species has also been found in the section of the Subglacial Canyon in the eastern part of the island, described above, where it occurs in the assured upper part of the Unit. However, at two points (samples 224/1 and 224/2) in the eastern part of the Three Streams outcrop another complex of graptolites appear, indicating (with high probability) the Middle Ordovician age of the host rocks, namely, that they belong to the *Corymbograptus deflexus* Subzone of the *Isograptus gibberulus* Zone of early Dapingian age (Webby et al. 2004). These samples were collected from a poorly exposed part of the section, and we do not exclude the presence of a fragment of the uppermost part

of the Middle Unit cropping out due to displacement by fault in the eastern part of the outcrop, exposed nowhere else on the island.

4.d.2. Northern Central Valley

From the saddle between the Toll glacier and the eastern De Long glacier to the south and NW, two rivers form wide valleys. We called them the Southern Central and Northern Central valleys (Fig. 2). The valley widens to about 1 km in the lower reaches of the northern river, merging in the western part with another valley filled with the outlet glacier. The glacier does not reach the sea, and the Ordovician rocks are exposed in the banks of the stream running from it (Fig. 16, Supplementary Fig. S10). Outcrops up to 0.7 m in height are traced in the sides of the brook for 300 m (between points 170 and 171) and occasionally occur upstream. The Ordovician rock scree with local outcrops was also found on a nearby hill. These exposures were not previously known.

The Ordovician rocks within the Northern Central Valley resemble carbonate flysch east of the Four Crates River, although interbedding is finer (centimetre scale). Massive calcareous siltstone beds contain small pyrite concretions (0.5–1.0 cm). Cross-stratification, convolute and horizontal lamination are present. At least 20 m of the section is exposed in the stream. Estimating the total thickness of the Ordovician deposits in the area is not easy, because dip direction changes over a short distance and outcrops are discontinuous. In addition, the Palaeozoic deposits are cut by dykes and stocks of the Lower Cretaceous dolerites, some of which are clearly confined to faults. The Ordovician rocks can be traced to a height of 80 m (point 259) along the slope, where basalts rest upon them. Presumably, the total visible thickness of the Ordovician deposits in the area is several tens of metres. On the slope the rocks are coloured in red and green, which is due to changes in the weathering crust and the thermal impact of the intrusions. The rock composition in the talus is the same: limestones with cross- and convolute bedding, mudstones and calcareous mudstones.

To the west of the outcrops described above, another small fragment of the Ordovician section (several metres) is exposed between points 172 and 173 in the lower part of the cliff. The rocks here are also coloured and overlain by the basalts.

Graptolites have been found at two points in this locality, characteristic of the *T. approximatus* Zone of early Floian age (samples 171/2, 171/3, 259/1; see Table 1). We assume that the rocks exposed in the Northern Central Valley correspond to the lower part of the carbonate turbidite Unit, perhaps to an unexposed interval at the mouth of the Four Crates River.

4.e. Summary of the Middle Unit: thickness, age and depositional environment

The sedimentary succession of the Ordovician Middle Unit of Bennett Island demonstrates a gradual transition from basal black shales to turbidites. Carbonate material apparently originated from a shallow-water part of the basin. Data on the overlying Unit indicate that the clastic material was transported from the NNE (present-day coordinates), where a carbonate platform (or possibly a ramp) might be located.

The carbonate flysch, which is the principal lithology of the Middle Unit, demonstrates sedimentary structures typical of low-density (distal) turbidite currents (Lowe, 1982). Rhythms contain Tb–Te divisions in terms of Lowe (1982), but lower parts including Tb or Tb+Tc are often reduced. Convolutions and other



Fig. 7. (Colour online) General view of the 318–114 exposure (SE is to the right; see Figs 2, 3). Cliff is up to 140 m high, and its lower part comprises Ordovician carbonate turbidites. The upper part of the cliff comprises lower Cretaceous basalts underlain by soft sediments (terrace). This outcrop was studied at the beginning of summer before the sea ice broke up.

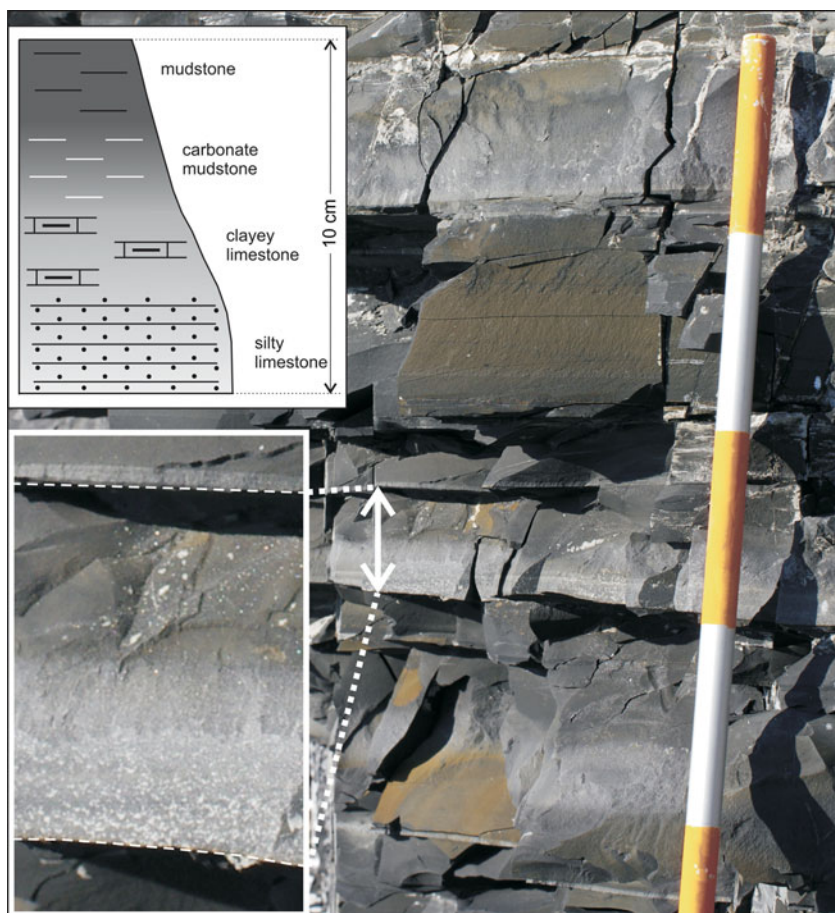


Fig. 8. (Colour online) Typical rhythm of carbonate turbidite. Each segment of range pole is 10 cm in height. Left: enlarged photograph of a single rhythm; upper left: drawing of this photograph.

soft-sediment deformations are quite noticeable features of the Unit. They were attributed to rapid sedimentation, which caused loading, liquefaction and water-escape processes along with flow-induced shearing and frictional drag (Stow, 2012). The convolute structures are usually associated with current ripples and contain relics of ripples as well as disturbed ripples, sunk in underlying sediment (Figs 11b, 15a; Supplementary Fig. S11). These observations and the transition from cross-lamination to convolute lamination from bottom to top in some layers confirm the idea

of PH Kuenen in 1953 (McClelland *et al.* 2011) that convolute folds nucleate upon ripples. Convolutions in the studied sections tend to overturn downstream in accordance with the orientation of the ripples.

We did not take mass measurements of current ripple cross-stratification because laminae do not exfoliate in carbonate rocks and true tilt orientation can be seen only if the bed is cut off in two directions. Available reliable readings have been found to be non-uniform, requiring a large number of measurements for statistical



Fig. 9. (Colour online) Carbonate siltstones (light grey) with sharp bottoms and tops, intercalated with dark-grey mudstones. In the lower part of the picture (below pole) is a marker bed of grey limestone with slump folds. Range pole is 2 m high.

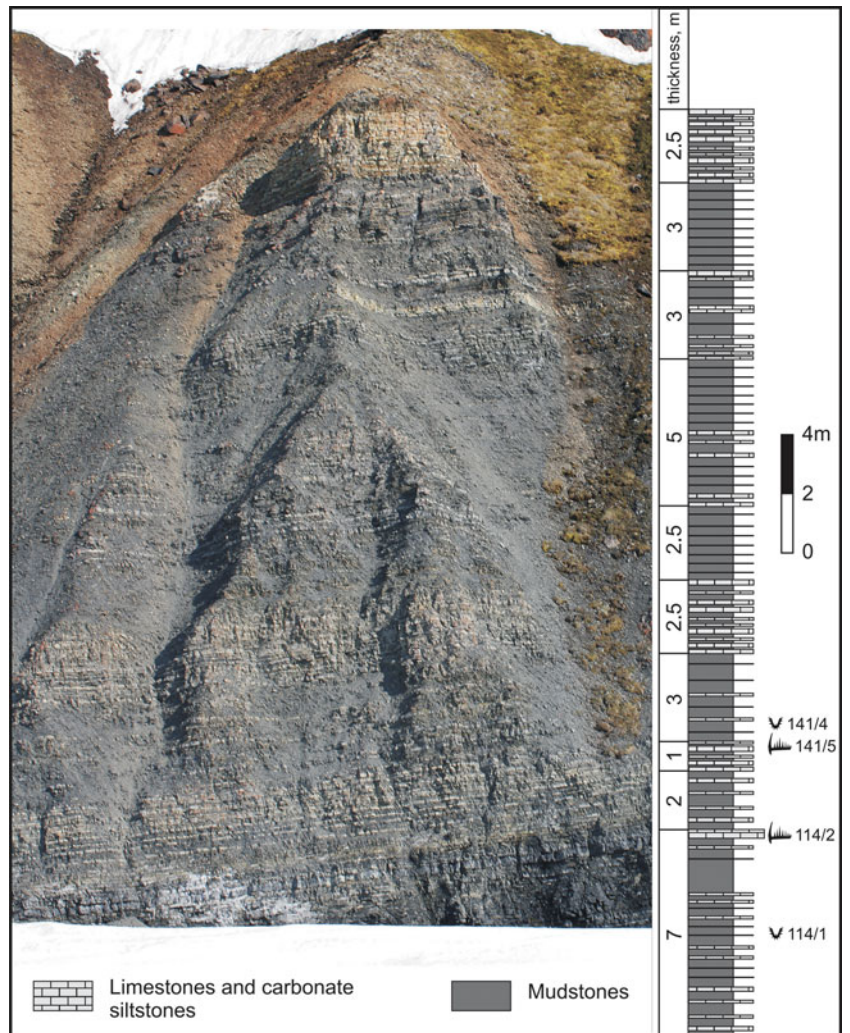


Fig. 10. (Colour online) Field photograph of the lower part of the carbonate turbidite Unit, visible in SE part of 318–114 exposure (near point 114), and respective column (at approximately the same scale). The total thickness of the fragment is 31.5 m; the lowermost several metres are shown only on the column. This section is divided into two types of packages: one is composed mainly of mudstones and the other contains many carbonate siltstone beds. A marker bed of grey limestone (see Fig. 9) is visible in the lower part of the photograph. Black lines in the column correspond to thin interbeds of siltstones, carbonate siltstones and limestones. Graptolite and conodont samples are shown on the right.



Fig. 11. (Colour online) Some types of sedimentary structures in carbonate turbidites exposed in the Subglacial Canyon: (a) convolute lamination in a clastic limestone; (b) current ripples sunk in underlying mud during silt accumulation; current direction was from right to left; (c) HCS-like structures with small hummocks and swales in calcisiltites of Subglacial Canyon (left: note the soft-sediment deformations).

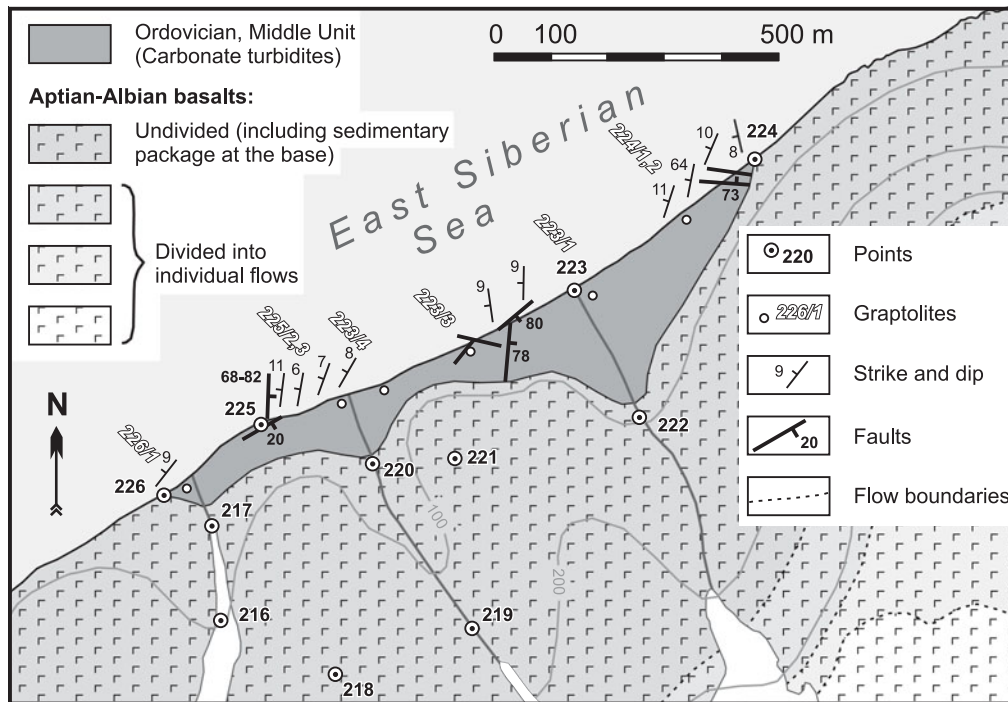


Fig. 12. Geological map of the best Ordovician exposure in NW Bennett Island, Three Streams locality. Glaciers and snow patches are shown in white.

Fig. 13. (Colour online) General view of the carbonate turbidites Unit exposure along the NE shoreline of Bennett Island (Three Streams locality). The Ordovician flysch is overlain by the Lower Cretaceous basalts. Contact occurs at an altitude of 50 m (right) and goes down to the sea level at the eastern end of the exposure (left). Cliff is 300–350 m in height.



Fig. 14. (Colour online) Contrast intercalation of carbonate sandstones and siltstones (light grey) with mudstones and siltstones (dark grey). Hammer is on the top of the bed with HCS-like lamination.



calculations to estimate the slope orientation. This non-uniformity may indicate reworking of the sediments by non-turbidite bottom currents.

Small-scale HCS-like structures have been observed in several beds within the carbonate flysch in the Subglacial Canyon and Three Streams area (Fig. 11c; Supplementary Figs S4, S8). They do not contradict the turbidite interpretation of the whole sequence. Such structures have been found in the Upper Cretaceous carbonate turbidites of the Western Pyrenees, and were described in detail by Mulder *et al.* (2009). These authors relate HCS-like beds to standing waves caused by Kelvin–Helmholtz instability at the upper interface of the turbidity current. In our scarce examples, there are only few elements resembling HCS. Relatively distinct hummocks and swales are shown in online Supplementary Figures S6 and S8A. Undulating erosion surfaces occur in other cases, and laminae also undulate but the general trend is unidirectional (Fig. 11c; Supplementary Fig. S4). Such

structures (as well as combined flow-like ripples; Supplementary Fig. S8B) could have been formed under the unidirectional-dominant flow but with some oscillatory component. The latter could appear due to the above-mentioned standing waves. Soft-sediment deformations were another process that affected the final geometry of HCS-like structures. For example, some features in Figure 11c show a similarity to convolute lamination and could originate from a syn-sedimentary folding.

The thickness of the Middle Unit in the southeastern part of the island is not less than 220 m. Its lower half contains the early Floian graptolites. The upper half of the Unit starts with mudstone of thickness 20–25 m with sparse limestone beds. Near the base it bears graptolites, coeval with graptolites from the lower half of the Middle Unit (*T. approximatus* Zone). This package is overlain by about 90 m of normal carbonate flysch with middle Floian faunas in the lowermost part and an upper Floian fauna 10 m above the base and in the upper visible part of the section. The uppermost

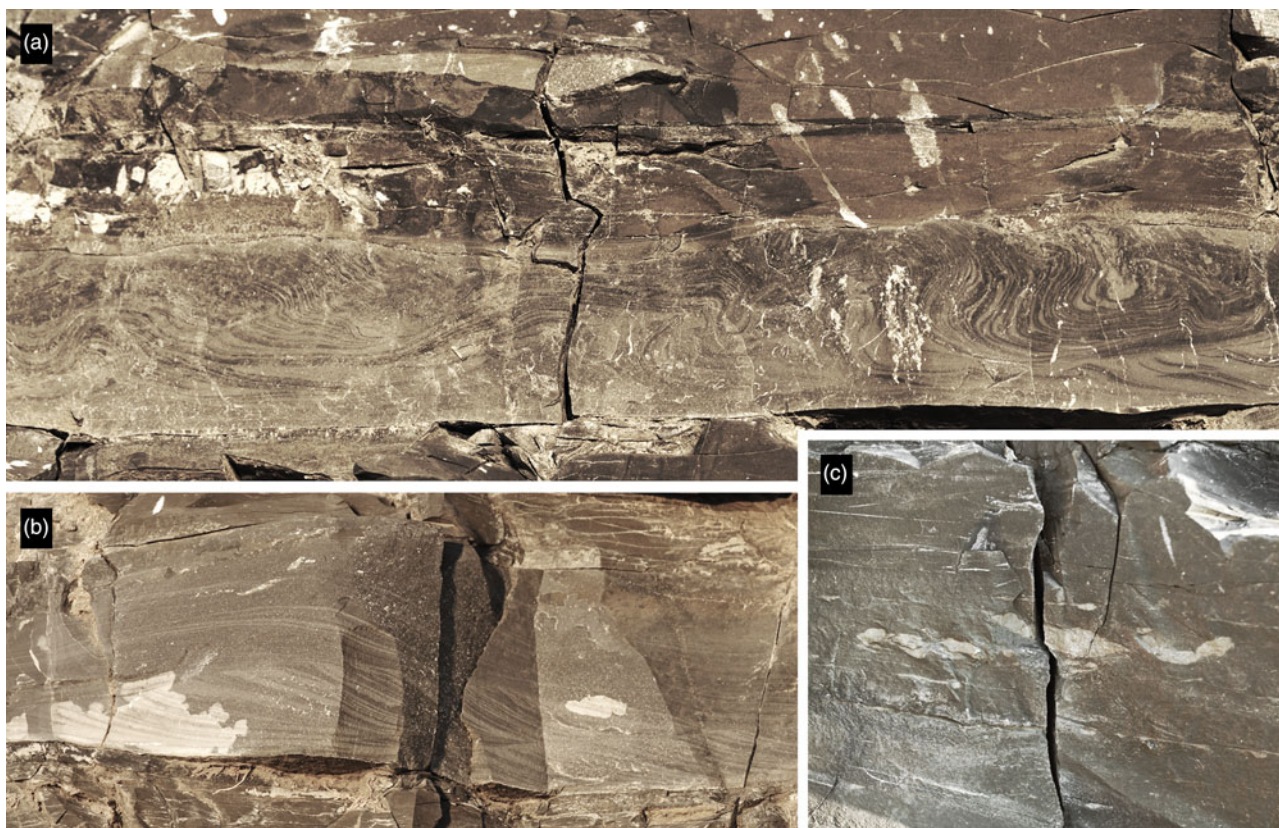


Fig. 15. (Colour online) Sedimentary structures in carbonate flysch, Three Streams locality. (a) Carbonate siltstone bed with convolute lamination and erosion top. Lens of siltstone in the upper part may be a current ripple sank into mud. The chain of such lenses can be seen in exposure (outwith the photograph, which is 12 cm high). (b) Climbing ripples at the base of carbonate siltstone (photograph is 15 cm high). (c) Sandstone nodules in dark-grey mudstone (photograph is 17 cm high).

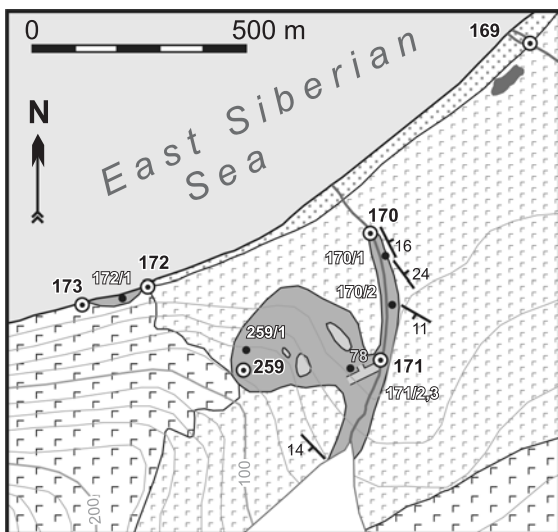


Fig. 16. Geological map of the Northern Central Valley locality. For legend see Figure 3. Cretaceous dolerite intrusions are shown in light grey, and white indicates glacier.

part of the Unit does not crop out in the area. The thickest portion (110 m) of the Middle Unit in the west of the island is entirely composed of carbonate flysch and is not older than of late Floian age. The total thickness of the Unit is therefore at least 250 m. Early

Dapingian graptolites in the deformed eastern end of the Three Streams exposure suggest that several tens of metres should be added to the above estimation.

5. Upper Unit: siliciclastic turbidites (Dapingian – lower Darriwilian)

The major part of eastern Bennett Island comprises siliciclastic turbidites that belong to the Upper Unit of the Ordovician System. These are the youngest Palaeozoic deposits exposed on the island. The Unit crops out in the cliffs of Pavel Keppen Bay between Cape of Transfiguration and the Lagernaya River (Fig. 3). Sides of the Lagernaya and Tollevskaya River valleys are covered with talus of the Ordovician rocks.

The Upper Unit is rather monotonous. Three types of rock intercalate in it: light-grey mud-poor quartzose sandstone with some carbonate grains and bioclastics; dark-grey unlaminated muddy sandstone (diamictite); and dark-grey to black mudstone, including a sandy variety. The sandstones of both types form individual beds (several decimetres, occasionally up to 2 m) separated by mudstone. They also participate in a thin-bedded (several millimetres to several centimetres) alternation with mudstone. Such intercalation sometimes forms distinct packages (‘black packages’) dominated by mudstone or muddy sandstone up to 10 m thick. Light-grey quartzose sandstone may also dominate at some intervals, comprising packages up to 15 m thick. Such sandstones exhibit distinct succession of sedimentary structures (from the

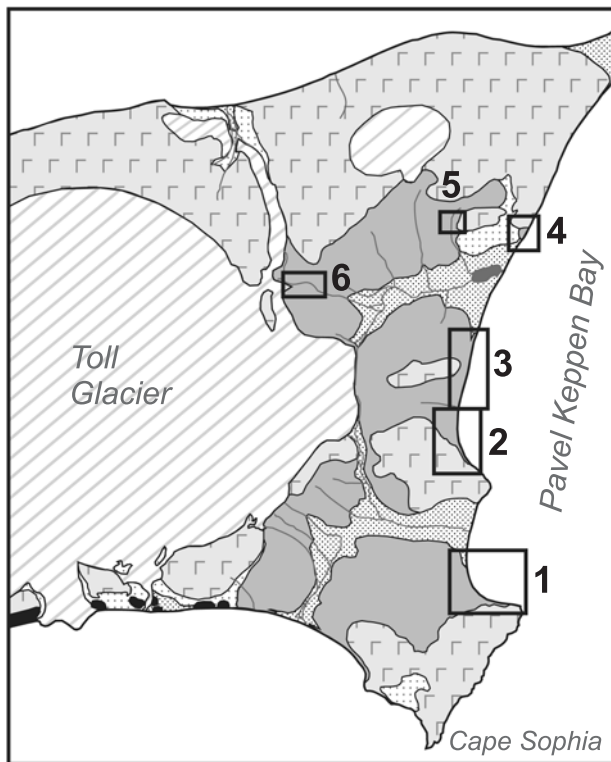


Fig. 17. Location of the Ordovician Upper Unit outcrops in the eastern part of the island. 1, southern exposure; 2, key exposure, southern segment; 3, key exposure, northern segment; 4, uppermost part of the Ordovician section; 5, local rocky outcrop near point 297; 6, outcrop near the foot of Toll glacier (points 299–300). Uniform grey shading corresponds to Ordovician rocks.

bottom to the top of an individual bed) typical of classical turbidites, namely the Bouma divisions.

Some parts of the Unit (more than 400 m in total), including its bottom, are not exposed in the cliff. The lower boundary was observed only in talus. The first good outcrop of the siliciclastic turbidites is located in the cliff between Cape of Transfiguration and the Tollevskaya River mouth (exposure 1 in Fig. 17). The thickness of the underlying poorly exposed portion of the Unit is about 95 m by geometric estimation. The extensive Ordovician cliff between the Tollevskaya and Lagernaya rivers, our reference section, is subdivided into two segments: southern and northern (exposures 2 and 3 in Fig. 17). The uppermost visible part of the Ordovician succession was observed in the cliff to the NW from the Lagernaya River mouth (exposure 4 in Fig. 17). In addition, there are some local rocky outcrops of the Unit in the Lagernaya River basin (exposures 5 and 6 in Fig. 17) and small outcrop in the west of the island (exposure 1 in Fig. 2).

5.a. Locality 1: southern exposure

Southwards of the Tollevskaya River mouth, the Ordovician rocks crop out in a 70–80 m high cliff. Closer to the Cape of Transfiguration, they are overlapped by the Cretaceous basalts along an uneven inclined boundary (Fig. 18). At the very cape, the cliff is composed of basalt columns 100 m high. The visible bottom of the Ordovician strata was examined at point 129 (Fig. 3). Here, near the contact with basalts, they are coloured in yellow, greenish and reddish dyes. From point 130 to the NW the rock colour is normal. About 80 m of the section is exposed in this locality;

part of it (52 m) has been measured with a range pole (Fig. 19). The visible succession can be divided into several members due to the sandstone and mudstone proportions. During fieldwork, the section (along with the other Unit exposures) was divided into a number of short intervals that are also shown in the column (Fig. 19): pole 1, pole 2, etc. Note that these intervals do not correspond exactly to a 2 m pole.

Member 1 (19 m) is dominated by beds of light-coloured sandstone (up to 1.2 m) separated by thin interlayers of mudstone or ‘black package’ (Fig. 20). Some amalgamated sandstone beds can split into two or three, being divided by mudstone. Mudstone layers usually have variable thickness due to erosion by subsequent turbidity current, loading of overlying sand, or slumping of semi-liquid sediment. The central parts of some sandstone beds contain carbonate concretion-like horizons, as well as indistinct horizontal lamination. In one of the layers (pole 4 in Fig. 19), slump folds were recorded (Supplementary Fig. S12).

Member 2 is the thickest (13.5 m) ‘black package’ in the Unit (Fig. 21). A layer of dark muddy sandstone 0.7 m thick with slump folds lies 2 m above its base. Such folds are oriented in a similar way throughout the Unit; the beds slipped from the NNE–NE to the SSW–SW.

Member 3 (11 m) is a relatively uniform alternation of all three main types of rocks. At the base there is a muddy sandstone covered with a noticeable bed of quartzose sandstone with large load marks (Figs 19, 21). The interval is rich in sedimentary structures inherent to turbidite. These are different types of stratification (horizontal, cross-, convolute; see details in Section 5.g), sole marks (Supplementary Fig. S13), rip-up mudstone clasts in sandstones and slump structures.

Member 4 comprises the second sandstone package (5.9 m). Some of the sandstone beds are amalgamated. The thickness of individual layers reach 1.8 m.

The lower Dapingian graptolites (*I. gibberulus?* Zone) were found in the lower part of member 1 (sample 129/1; see Table 1 and Fig. 19). A few Dapingian graptolites were also collected from different horizons of member 2 (130/2, 130/2a).

The overlying strata in this cliff segment resemble that of member 3. Their thickness is calculated from the photographs as c. 30 m. They reveal distinct cyclicity; in the lower part of each cycle the number and thickness of the light-grey sandstone beds are low, but these grow upwards. Over a cycle, thickness varies from 1.5 to 6.0 m. Graptolites from near the base of this 30 m interval (sample 134/1) are poorly preserved and characteristic of the Lower–Middle Ordovician System.

5.b. Locality 2: key exposure (southern segment)

No Ordovician rocks crop out between the southern exposure and the beginning of the key exposure (Fig. 3, point 135). The unexposed interval has a thickness of not less than 150 m (estimated geometrically). The middle part of the key exposure is cut by a large ravine (point 103, Fig. 3) that divides the cliff into two segments: the northern and southern segments. At least 87 m of the section crops out in the southern segment (Fig. 22).

The rock composition of the lower 19 m of the section exposed between points 135 and 136 is shown in Figure 22. The sedimentary structures here do not differ from that in the southern outcrop, but their preservation is poorer since the rocks were altered in a weathering crust.

The interval of cliff 136–137 is disrupted by a series of normal E–W-striking faults. Their southern walls are sunk, meaning that

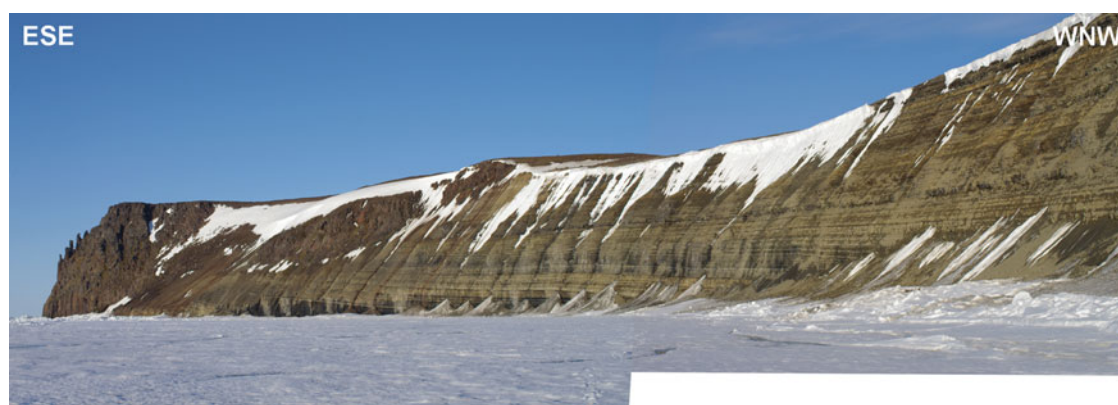


Fig. 18. (Colour online) Lower part of the Upper Unit visible in cliff. Cape of Transfiguration is on the left.

some parts of the sequence crop out twice (e.g. pole 1b–pole 2b in Fig. 22). Collected graptolites (sample 136/1, Table 1) show a wide stratigraphic distribution (Dapingian).

At point 137 the section is disrupted by the last fault in the series. The pattern of intercalation on the opposite walls does not correlate, so its amplitude exceeds 20 m. Further north to point 103 another 68 m of the section is exposed, comprising a continuous homocline. This segment of the section was divided into the 10 members depicted in Figure 22. The composition of some intervals is shown in photographs (Fig. 23; Supplementary Figs S14–S16). Notably, members 3 and 5 are dominated by dark diamictitic sandstone (Fig. 23; Supplementary Fig. S14). Lenticular bedding and slump folds are observed in member 5. This cliff segment is remarkable for well-preserved typical turbidite features such as sandstone stratification, dewatering sheets, amalgamation of beds, sole marks and carbonate concretions (Supplementary Figs S17, S18).

The upper part of member 4 contains graptolites (sample 137/1) characteristic of the *Isograptus maximo-divergens* Subzone of the *I. gibberulus* Zone of early Dapingian age (Loydell, 2012). The graptolites of a similar zone are also found at the top of member 7 (sample 138/3). Lower–Middle Ordovician graptolites (sample 138/4) were collected from the different horizons of the interval pole 17 (Fig. 22; the upper part of member 8 and lower part of member 9).

5.c. Locality 3: key exposure (northern segment)

A continuous part of the Ordovician section carries on to the north of point 103, and is subdivided into 11 lithological members here (Fig. 24). Bed 1 (the base of member 1) occurs above pole 21 of the previous section (the top of respective member 10). The total thickness of the section in the northern segment of the key exposure is 110 m.

In locality 3 no significant changes in relation to the underlying sequence has been observed (Fig. 17), but the following can be noted. While light-grey sandstones generally predominate in localities 1 and 2, their proportion in the northern segment of the key exposure, likewise the thickness of individual beds, decreases. A significant role is played by the dark muddy sandstone. Member 3 is particularly interesting, as a 2.3 m thick diamictitic sandstone occurs at its base (Supplementary Fig. S19). It is the thickest bed of this kind in the Ordovician section. Another interval of the section, exceptionally rich in dark sandstones, is member 6 (Fig. 24). Here and at other levels of the section, slump folds,

disrupted fragments of laminated sequences and mudstone clasts (Supplementary Fig. S20) and ball-and-pillow structures are all observed (Supplementary Fig. S21). The muddy sandstone occasionally grades upwards into mudstone.

Member 5 (Fig. 24) represents a 20 m interval in which ‘black packages’ predominate. This member resembles the middle part of the section in locality 1 (member 2 in Fig. 19) but, unlike in locality 1, it contains a number of noticeable (the first decimetres thick) beds of dark sandstone and, less often, light-grey sandstones.

In the Ordovician section at this locality, the volume proportion of quartzose sandstones, dark muddy sandstones and mudstones is generally approximately equal. Rocks demonstrate the same set of sedimentary features as in the underlying strata. In particular, many beds of light-grey sandstone show normal grading and a sequence of rhythm elements typical of turbidite (Fig. 25). In sandstone-rich member 10, clear dewatering structures are particularly characteristic (Fig. 26).

Graptolites of assumed Dapingian – earliest Darriwilian age (Fig. 24; Table 1) were found at a number of levels of the section. These include both species of wide stratigraphic range and zone (given below). Samples from members 1 and 2 contain species characteristic of the *I. gibberulus* Zone of early Dapingian age. Notably, one sample (138/1) include taxa of the *I. maximo-divergens* Subzone. A complex of graptolites from the top of member 5 (sample 108/7) characterizes the upper Dapingian deposits (*Expansograptus hirundo* Zone). A rich complex of graptolites (sample 323/1) was found in the middle of member 11 likely characteristic of the same zone; alternatively, it may be attributed to the upper Dapingian – lowest Darriwilian deposits. In addition, a sample of calcareous sandstone from the southern slope of the Lagernaya River valley (Fig. 3) revealed numerous conodonts of early Darriwilian age (sample 313/1). Tracing this level on the map shows that it roughly corresponds to the very tops of the key section, or slightly higher.

5.d. Upper horizons of the Ordovician section

The uppermost part of the Ordovician section exposed on the island was examined NE of the Lagernaya River mouth in a small portion of a cliff between points 320 and 102 (Fig. 3). A wide beach stretches for c. 2 km between the northern end of the key section and point 320. The calculated thickness of the unit unexposed in the cliff is 180 m. Judging by the rock fragments on slopes of the Lagernaya River valley, this part of the section comprises the same turbidites as in the cliffs to the north and south of the river mouth.

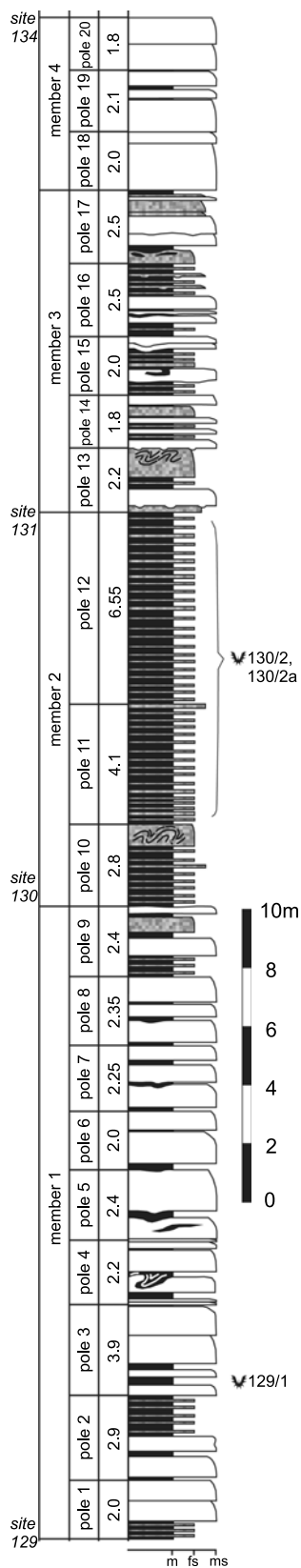


Fig. 19. Measured section of siliciclastic turbidites near the Cape of Transfiguration (southern exposure). The section was divided into short intervals ('poles') during field-work, which are shown here with corresponding thickness in metres. Members described in the text are shown in the left column. Grain size (below the column) abbreviations: m – mudstone; fs – fine-grained sandstone; ms – medium-grained sandstone. Graptolite samples are displayed to the right of the column. For legend see Figure 22.

A small fragment of the section (2.3 m) is seen near point 320 in a low scarp, and a larger part of the section crops out between points 321 and 102 (10–15 m in thickness; Supplementary Fig. S22). The composition of the Ordovician upper horizons is similar to that in the key section: two types of sandstones interbedded with mudstones and 'black packages'. However, in contrast to the main part of the key section, here the light-grey sandstone beds are usually thin (7–15 cm) but frequent. They demonstrate a common set of poorly preserved structures: planar, cross- and convolute lamination. At point 102, the uppermost Ordovician layers are overlain by Cretaceous rocks. The contact is disrupted and the upper horizons of the section are coloured and disturbed in the fault proximity. A large collection of graptolites (sample 102/1, see Table 1) was found in this part of the section; poorly preserved, they do not allow age determination more precisely than Dapingian – early Darriwilian.

5.e. Local outcrops in the Lagernaya River basin

In addition to the eastern cliff, the Ordovician rocky outcrops have also been found in two localities in the island interior in the Lagernaya River valley. One of them is situated near point 297 (Fig. 3). Slabs of weathered sandstones that plunge unexpectedly steep to ENE (20°) were encountered in the bed of temporary flow at the left slope of the Lagernaya River valley between 80 and 100 m asl. Over the major part of the key exposure, the homocline dips NE-wards at 7–10°. Perhaps rocks were tilted in proximity to a series of faults bordering basalts and associated with volcanotectonic subsidence. The sandstone slabs occur down the creek for about 70 m, but their thickness is insignificant.

The second locality is in the upper reaches of the Lagernaya River near the Toll glacier foot (points 299, 300 in Fig. 3). This site is unusual for the island: over a fairly large area (600 m along the river bed and on the neighbouring slope), the Ordovician rocks make up small ridges and quests, representing erosional remnants cut by furrows (Supplementary Fig. S23). The height of such remnants does not exceed 3–4 m. This relief was formed by subglacial water flows at a time when the glacier covered a larger area. Exposed sandstone and shale intercalation is typical for the Upper Unit and demonstrates similar sedimentary structures. Layers dip E-wards at 11–13°, the same tilt as that of the slope, and visible thickness does not exceed 20 m. Rocks in this locality can be traced on map to the lower–middle parts of the Upper Unit in the cliff. This is confirmed by Early Dapingian graptolites (*I. gibberulus* Zone) found near point 300 (sample 300/1).

5.f. Siliciclastic turbidites in the west of the island

The site is located at a barely accessible part of the island on the northwestern shore, 1.5 km from Emma Cape (Fig. 2). In this locality, the Lower Cretaceous coal-bearing deposits at the base of the basalts were mentioned by Vol'nov & Sorokov (1961), but the Ordovician strata were not visible at that time because of snow cover. We obtained access to the shore along a gully from the basaltic plateau (365 m high) by descending permanent snow patches covering vertical segments of the gully bed.

The Ordovician deposits are sporadically exposed in the lower part of the cliff between points 247 and 249 (Fig. 27). The rocks lie almost flat and dip 8° W-wards in the southwestern-most outcrop. The lower part of Ordovician cliff has a maximum height of c. 15 m (185 m SW of point 248). The total thickness of the visible section is no more than 30 m. The Ordovician deposits are altered in the



Fig. 20. (Colour online) Lower sandstone-dominated member at the base of the southern exposure section. Beds boundaries are wavy. Some sandstone beds contain leached carbonate concretions. Range pole is 2 m high.

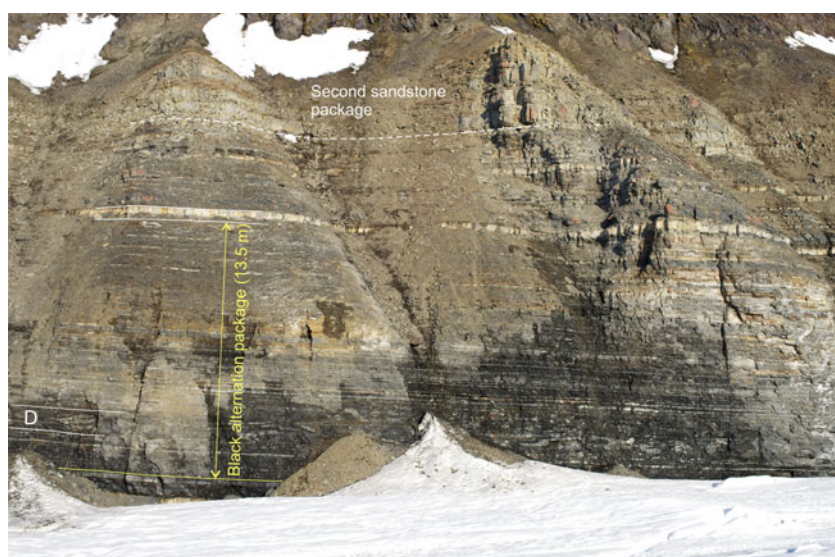


Fig. 21. (Colour online) Thick alternation package composed of mudstones and muddy sandstones with slump structures. The most impressive slump folds are present within 0.7 m thick diamictitic sandstone bed (D). In the upper part of the photograph, a second sandstone-dominated package (member 4, 5.9 m) of the southern exposure section is highlighted.

weathering crust and overlain by Cretaceous terrestrial coal-bearing sediments and basalts.

The Ordovician rocks on the site are unevenly interbedded shales and sandstones. The thickness of the latter reaches 1 m in the exposed top of the section (Supplementary Fig. S24). Primary sedimentary structures are not preserved as a result of weathering. Lower Dapingian graptolites (sample 249/1) typical of the *I. maximo-divergens* Subzone of the *I. gibberulus* Zone were found at point 249. In the east of the island, similar graptolites were found only in the southern segment of the key exposure (i.e. in the middle part of the Unit).

5.g. Summary of the Upper Unit: thickness, age and depositional environment

Light-grey mud-poor sandstones of the Upper Unit demonstrate a wide range of sedimentary structures that are usually considered to be typical of 'classic' turbidites of the Alps and Apennines (Mutti & Ricci Lucchi, 1978; Amy *et al.* 2005; Tinterri *et al.* 2012). Among them there are normal grading, dewatering structures and sole

marks (flute and groove casts, load marks). A complete set of lamination types in the sandstone beds (from bottom to top) corresponds to the Ta–Tc standard divisions of the Bouma sequence and can be described as non-stratified lower part, horizontal lamination, cross-lamination or climbing ripples, deformed cross-lamination and convolute lamination. Some members of this succession are often absent; photographs of the sedimentary structures are provided in Figures 25 and 26 and in Supplementary Figures S25–S27.

A considerable portion of the sequence is composed of unsorted structureless dark-grey muddy sandstones. Similar beds among turbidites were described in literature as debrites (e.g. Soh, 1989; Talling *et al.* 2004), sandy slump deposits (Shanmugam, 2012) or incompletely mixed slumps (Lowe & Guy, 2000). Such structureless rocks can also be the result of syn- to post-depositional liquefaction and fluidization (Pickering *et al.* 1995; Talling *et al.* 2004). Muddy sandstones in the studied sequence form distinct beds with sharp boundaries; transition to the overlying mudstone is rarely gradational. If overlying dark sandstones, light-grey turbidite sandstones demonstrate erosional lower contact. Muddy

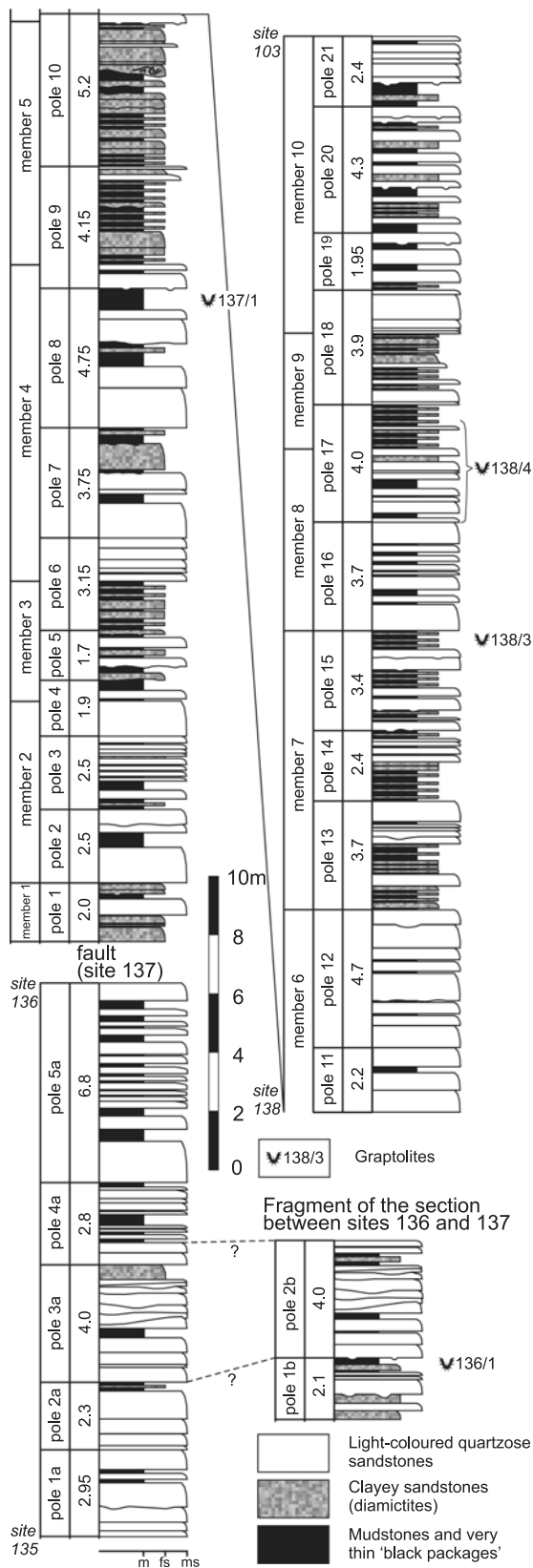


Fig. 22. Measured section of siliciclastic turbidites in southern part of the key exposure (between points 135 and 103). As in Figure 19, the section was divided into small intervals ('poles') during fieldwork, which are shown here with corresponding thickness in metres. Large intervals (members) are shown in left column. Granulometric bar (below the column) includes: m – mudstone; fs – fine-grained sandstone; ms – medium-grained sandstone. In legend: 'black packages' – thin-bedded alternation packages.

sandstones sometimes contain enclaves of deformed layered succession and/or mud clasts. The features listed indicate that these rocks are a result of mingling of sand, silt and clay during its downwards transport by debris flows. The latter were likely triggered by slumps and not by turbidity currents, as proposed by Talling *et al.* (2004). We did not observe any evidence that light-coloured and dark-coloured sandstones in the Upper Unit resulted from a single process.

Background sediments are represented by mudstones. Although there are many dark fine-grained rocks in the section, they are dominantly localized in the intervals of fine alternation of sand, silt and clay matter and their mixture ('black packages'). It may be assumed that a significant part of mudstones in these intervals was deposited from the residual suspension of turbidite flows, the major portion of which was discharged upslope. The 'black packages' also contain thin layers of specific sandy mudstone, in which coarse sand is mixed with a clay matrix. Surprisingly, some of these layers are rich in graptolites for an unknown reason. It is not always possible to recognize in the section intervals of pure background sedimentation, which occurs without precipitation from silty or clayey suspension stirred up by turbidity flows. Condensed beds of insignificant thickness (several millimetres to centimetres), whose surfaces were completely covered with multilayered graptolite remains, are undoubtedly related to background deposition.

The light-grey sandstones of the Upper Unit correspond to the sublithic arenites and, less often, to lithic arenites (Pettijohn *et al.* 1987; Supplementary Fig. S28). They are typically poorly sorted and contain some clayey-silty matrix. Some rocks have patchy carbonate cement, and grain size ranges from silt to coarse sand. A degree of roundness of clastic material is variable: coarse grains are usually well-rounded, while the fine fraction may contain angular fragments. Lithic clasts are limestones (some with silicate grains), cherts, quartzites and sparse magmatic rocks (basalts, felsites and micro-diorites, etc.). Fragments (up to several millimetres) of benthic fauna with a carbonate skeleton, evidently transported from shallow waters, and rare plagioclase and microcline fragments were revealed. The total amount of carbonate (debris and cement) in some rocks reaches 50%. The muddy sandstones contain a large amount of clayey-silty matrix (sometimes > 60%; Supplementary Fig. S28). Black organic matter and small flakes of a white mica often occur in matrix. Apart from that, the composition of the two sandstones is the same.

Zircon, mostly well-rounded, predominates among the heavy minerals in the sandstones. Euhedral crystals are scarce. The second most common mineral is tourmaline, also well-rounded. A significant amount of apatite is present. Garnet and epidote only occur rarely, but there is a small amount of biotite, chlorite and ilmenorutile(?). Such a composition of heavy minerals, along with the dominance of rounded quartz grains in the sandstones, indicates a maturity of the parental sediment, likely as a result of long transportation and/or reworking (e.g. in coastal-marine conditions) before it was involved in a turbidite flow. Matte surfaces of the rounded zircon grains may indicate an eolian transport. However, there was also a relatively proximal source of debris, as evidenced by presence of rare euhedral acicular zircon and apatite crystals, as well as fragments of volcanics and microcline. The source of these fragments could be granitoids and volcanic rocks (mafic and felsic), but its contribution was insignificant.

The orientation of the sole marks and slump folds in rocks of the Upper Unit indicates that siliciclastic material was transported into the Ordovician basin from the NNE (present-day



Fig. 23. (Colour online) Turbidite succession in the middle part of the southern segment of the key exposure. Dark alternation package with predominant muddy sandstones (upper part of member 3, see text) is in the lower part of cliff, overlain by 10.8 m thick quartzose sandstone package (member 4). Lithologic column is slightly deformed to fit the photograph and therefore not to scale. Range pole (encircled) is 2 m high.

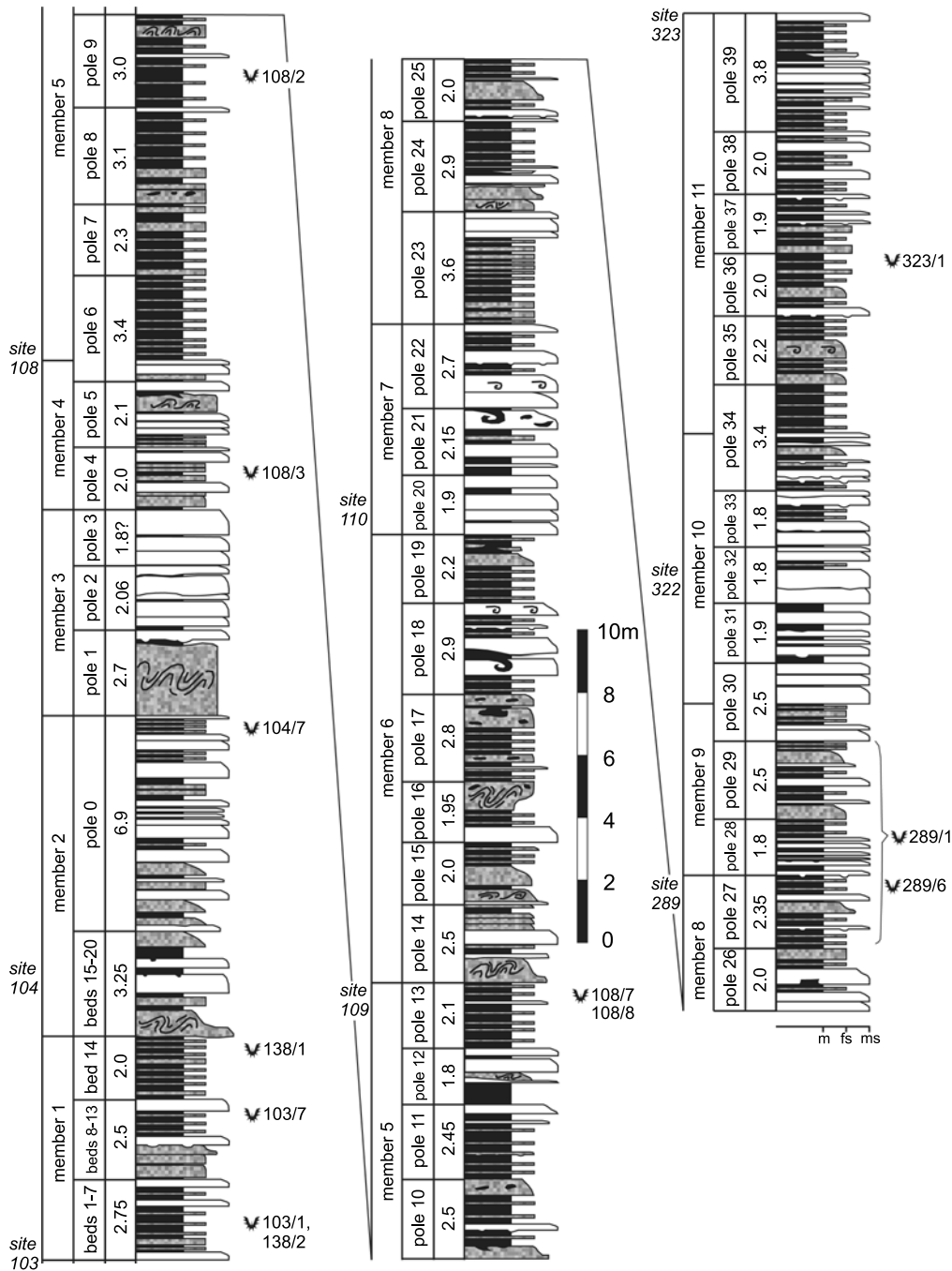


Fig. 24. Measured section of the siliciclastic turbidites in the northern part of the key exposure (between points 103 and 323). For legend see Figure 22.

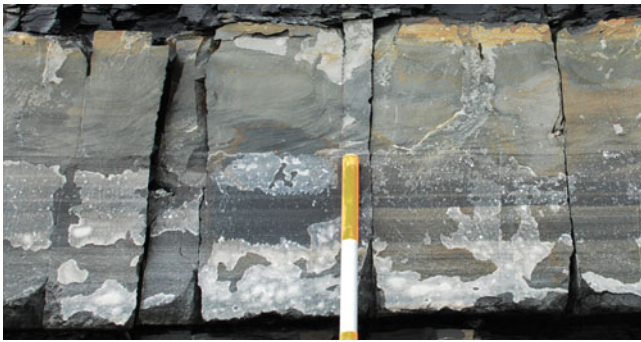


Fig. 25. (Colour online) One of the examples of complete sequence of sedimentary structures through sandstone bed (from bottom to top): poorly stratified lower part, horizontal lamination, cross-lamination, deformed (slump-like) cross-lamination. Note normal grading in this bed. The coloured section of range pole is 10 cm.



Fig. 26. (Colour online) Dewatering sheets in light-grey quartzose sandstone.

coordinates). It was apparently sourced from the land formed during early Dapingian time, NE of the present-day Bennett Island position. These issues will be discussed in the forthcoming paper concerning an interpretation of the detrital zircon ages.

The age of the Upper Unit is Dapingian – early Darriwilian. This is confirmed by recently published data: a complex of graptolites, typical of the late Dapingian – early Darriwilian period, was discovered during a geological excursion in 2011 in the top of the section (presumably corresponding to the upper horizons of the key exposure in our description), according to preliminary determination by RF Sobolevskaya (Vernikovskiy et al. 2013). The total thickness of the siliciclastic turbidite Unit is at least 730 m, and its composition is monotonous throughout the whole sequence.

6. Graptolites and conodonts of Bennett Island

6.a. Graptolites

Lower Palaeozoic graptolitic shales on Bennett Island were known of for a long time. The first graptolites were found by EV Toll and determined later by G Troedssen as *Didymograptus* sp., *Tetragraptus* sp. and *Phyllograptus* sp. (Ermolaev & Spizharsky, 1947). Fossils collected by MM Ermolaev, DA Volnov and DS Sorokov were identified by AM Obut as *Cryptograptus atenarius* (Hall), *Cryptograptus* aff. *hopkinsoni* (Nicholson), *Didymograptus murchisoni* (Beck), *Eoglyptograptus* cf. *dentatus* (Brongniart), *Tristichograptus ensiformis* (Hall), *Glossograptus* sp., *Gymnograptus* sp., *Leptograptus* sp. and the same genera as in Toll's samples (Sorokov et al. 1961; Obut, 1964; Sobolevskaya, 1976). Sobolevskaya (1976) identified additional

taxa from BS Klubov's collection: *Didymograptus* ex gr. *bifidus* (Hall), *Eoglyptograptus dentatus* (Brongniart), *Cardiograptus* aff. *crawfordi* Harris, *Glossograptus* aff. *acanthus* Elles et Wood, *Pseudoclimacograptus* sp., *Cryptograptus tricornis schaeferi* Lapworth, *Paraglossograptus* aff. *etheridgei* Harris and *Loganograptus* ex gr. *logani* (Hall).

Our collections have revealed the presence of the following graptolite zones on the island: *T. approximatus* (this zone is known in many countries, e.g. in Sweden in the global boundary stratotype section and point or GSSP of the Floian Stage lower boundary; Bergstrom et al. 2004; Loydell, 2012); *P. densus* (this zone is known in many countries, including Baltoscandia; Webby et al. 2004); *D. protobifidus* (this zone is known in Australia; Loydell, 2012), *I. gibberulus* (this zone is known in many countries, including Britain; Zalasiewicz et al. 2009; Loydell, 2012); *E. hirundo* (this zone is known in many countries, including Britain and Baltoscandia; Webby et al. 2004; Loydell, 2012); and *U. austrodentatus*(?) (this zone is known in many countries, e.g. in China in the GSSP of the Darriwilian Stage lower boundary; Mitchell et al. 1997; Webby et al. 2004; Loydell, 2012) that belong to Floian, Dapingian and Darriwilian (Figs 28, 29; Table 1). Available data on neighbouring regions, such as the Siberian platform (Sennikov, 1996, 1998), Taimyr (Obut, 1964; Obut & Sobolevskaya, 1964; Koren' et al. 2006; Sobolevskaya, 2011) and Kolyma regions (Obut & Sobolevskaya, 1964; Sobolevskaya, 1969, 1971, 1973, 1974; Koren' et al. 2006), show that the Bennett Island Ordovician succession has the most detailed sequence of graptolite assemblages. Bennett graptolite assemblages are also characterized by a rather diverse taxonomic composition (both genera and species). All graptolites species are of wide geographical range.

6.b. Conodonts

Conodonts have been found at two stratigraphic levels. The first assemblage was obtained from a marker bed of grey limestone in the middle part of the Middle Unit (sample 114/2; 318–114 exposure; Figs 3, 4, 9, 10), in which elements of the species *Oepikodus* cf. *intermedius* (Serpagli), *Protoprioniodus papillosus* (van Wamel), *Paracordylodus gracilis* Lindström, *Kallidontus corbatoi* (Serpagli), *Cornuodus longobasis* (Lindstrom), *Acodus* sp., *Drepanodus* sp. and others (Fig. 30a–s) were found. The assemblage is strongly dominated by elements of *Oepikodus intermedius*, which constitute c. 80% of all elements. A set of species is characteristic of the upper Floian (lower parts of the *O. evae* Zone) Lower Ordovician deposits (Lofgren, 1994; Wang et al. 2005; Wu et al. 2010). Similar, but much scarcer, conodonts were extracted from silty limestone 3 m upsection (sample 141/5).

Conodonts of the second stratigraphic level were found in the upper half of the Upper Unit (sample 313/1; Lagernaya River valley; Figs 3, 4) in carbonate nodule from sandstone. Among them are *Paroistodus horridus* (Barnes et Poplawski), *Periodon* cf. *macrodentata* (Graves et Ellison), *Spinodus spinatus* (Hadding) and single, indefinable elements of the genera *Polonodus*, *Ansella*, *Scolopodus*, *Acodus* and *Costiconus*. These conodonts are characteristic of the early Darriwilian age (Fig. 30t–w) (Pyle & Barnes, 2002; Serra et al. 2015).

The age of both complexes of conodonts has been confidently determined, since all the taxa found in the Floian and Darriwilian deposits of Bennett Island are species of a wide geographical distribution and are present in the deep-sea sediments of many continents. They are known from Kazakhstan (Tolmacheva, 2014), Newfoundland (Stouge, 1982; Pohler, 1994) and the Canadian

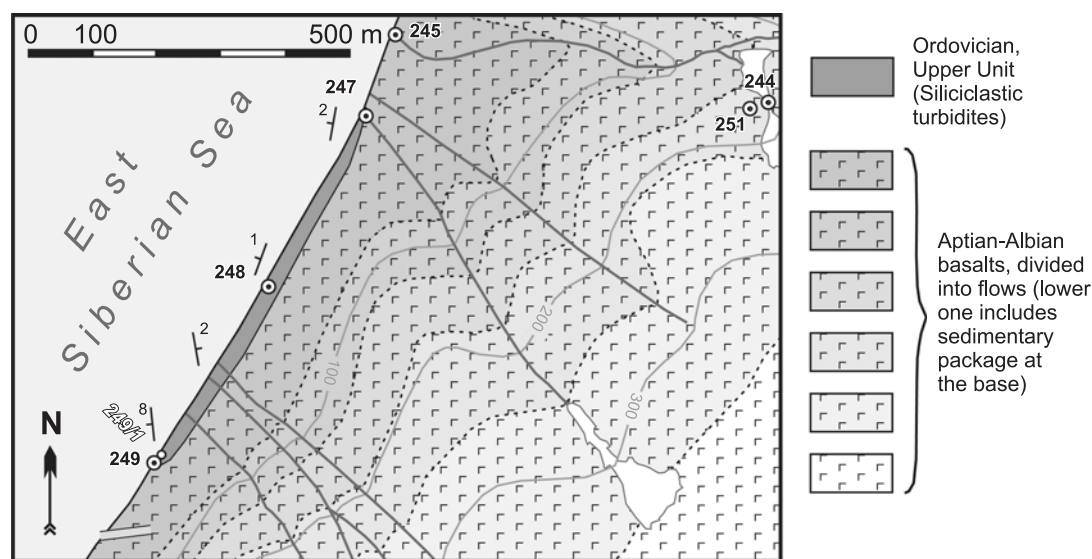


Fig. 27. Geological map of the westernmost Ordovician exposure on Bennett Island. For legend see Figure 12. Cretaceous dolerite dyke is shown in light grey and white indicates snow patches.

Arctic (Pyle & Barnes, 2002, 2003). The shallow-water taxa that would indicate palaeogeographic proximity to any continent are absent from the studied assemblages. In particular, no taxa characteristic of shallow-water deposits of the Siberian or North American platforms were found.

The only possible assumption about the palaeogeographic location of the Bennett palaeobasin is that it was situated in a warm-water, likely equatorial, climatic zone during Floian and Darriwilian time. This is indicated by the presence of species *K. corbatoi*, *O. cf. intermedius* and *P. horridus*, which are absent from the deposits of the Balto-Scandian palaeobasin of the northwestern part of the East European Platform (Lofgren, 1994; Rasmussen, 2001; Mannik & Viira, 2012), located at relatively high latitudes.

7. Lower and Middle Ordovician rocks in other Eastern Arctic regions

The Ordovician rocks are widespread in the Eastern Arctic, providing the possibility of correlations. A well-known comparison of the lower Palaeozoic rocks, with much focus on the Ordovician System, was published by Dumoulin *et al.* (2002). New data on Bennett Island may reinforce circum-Arctic correlations.

7.a. Kotel'ny Island

The Ordovician is the oldest known division in Kotel'ny Island (Fig. 31). It comprises a lower part of a thick shallow-marine carbonate succession, which includes Silurian and Lower–Middle Devonian deposits. The lowermost exposed unit (part of Lower Ordovician and lower Middle Ordovician strata, up to 650 m) consists of dolostones, algal and subordinate bioclastic limestones (Fig. 32). These carbonate rocks often contain silt-sized silicate clastics. Wave ripples, mud cracks, thin horizontal lamination and cross-stratification are common (Kos'ko *et al.* 1985). Conodonts of late Tremadocian – early Floian age have recently been revealed in the middle portion of this unit (Vernikovskiy *et al.* 2013). The upper part of the Middle Ordovician – lower Upper Ordovician deposits (290–620 m) is made of grey-coloured

limestones (including bioclastic limestones), clayey limestones and minor mudstones. Various benthic faunas are abundant in some sections.

The Ordovician – Middle Devonian sequence in Kotel'ny Island was interpreted by Şengör & Natal'in (1996) as a part of the New Siberian carbonate platform, whose other parts crop out in NE Chukotka and northern Alaska where they demonstrate the same age and lithology. However, we believe this platform was not isolated as the authors proposed, but was attached to the Siberian Platform. This interpretation is supported by a strong resemblance of the Kotel'ny Island Ordovician–Silurian facies and faunas to that of the Southern Taimyr (Danukalova *et al.* 2015). The same is observed in the Early–Middle Devonian facies and faunas (Cherkesova, 1975; Nekhorosheva, 1977). The Southern Taimyr domain was already adjoined to the Siberian continent during early Palaeozoic time (see below). Early–middle Palaeozoic faunal assemblages of northern Siberia and Kotel'ny Island also have much in common.

7.b. Southern and Central Taimyr

The Taimyr Peninsula is usually subdivided into three tectonic zones that are aligned in the NE–SW direction (e.g. Bezzubtsev *et al.* 1986; Fig. 31). The Southern and Central Taimyr are separated by the Pyasina–Faddey fault. Both zones are considered by most geologists to be part of the Siberian continent from at least latest Neoproterozoic time (e.g. Vernikovskiy, 1996). The Northern Taimyr is bordered by the Main Taimyr thrust from the Central zone. The Northern Taimyr zone, together with the Severnaya Zemlya archipelago (see Section 7.e), is thought to belong to the Kara terrane that collided with Siberia during late Palaeozoic time (e.g. Nikishin *et al.* 2015). The Ordovician rocks in the first two zones demonstrate a transition from a shallow-marine carbonate-dominated succession in the Southern zone to distal and rather deep-water graptolitic shales and siltstones in the northern Central Taimyr (Fig. 32); both have been interpreted as the Siberian passive-margin deposits (Vernikovskiy, 1996).

While the Southern Taimyr carbonate succession has much in common with that of Kotel'ny (see Section 7.a), the lower

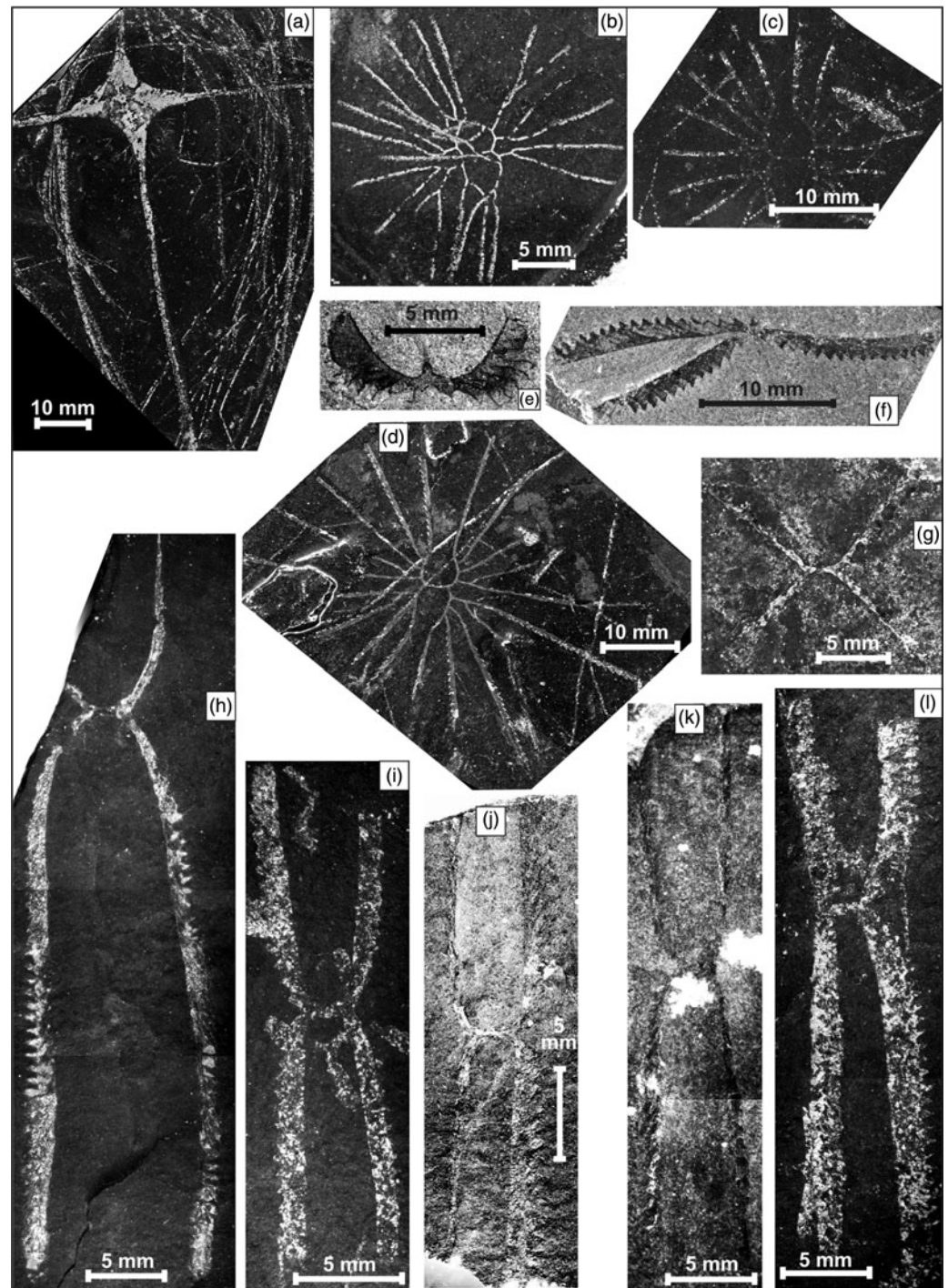


Fig. 28. Ordovician graptolites from Bennett Island. The collection of graptolites is kept at the GEOCHRON Core Facilities & Shared Resources Center of Geological (palaeontological, micropalaeontological and palynological) Materials & Collections for Siberia and Arctic regions, affiliated with the Trofimuk Institute of Petroleum Geology and Geophysics SB RAS (Novosibirsk; collection 2002). (a) *Eotetraraptus* ex gr. *quadribrachiatus* (Hall) (with large disc), location 108/8b. (b) *Loganograptus logani* (Hall) (2 rhabdosomes), location 136/1. (c) *Loganograptus logani* (Hall), location 103/7. (d) *Loganograptus logani* (Hall), location 108/7. (e, f) *Tetraraptus* ex gr. *biggsbyi* (Hall), location 140/1. (g) *Eotetraraptus quadribrachiatus* (Hall), location 279/1a. (h) *Paratetraraptus approximatus* (Nicholson), location 279/2. (i) *Paratetraraptus approximatus* (Nicholson), location 318/1. (j, k) *Paratetraraptus* aff. *acclinans* (Keble), location 281/1. (l) *Paratetraraptus* ex gr. *approximatus* (Nicholson), location 318/1.

Palaeozoic rocks of the Central Taimyr demonstrate some similarities with that of Bennett Island (Fig. 32). In both regions the upper Cambrian – Lower Ordovician (Tremadocian) black shales with subordinate carbonate rocks overlie the middle Cambrian (Mayan) variegated clay-carbonate unit (Danukalova *et al.* 2014). The younger part of the Central Taimyr Ordovician succession differs from that of Bennett Island. The Arenigian–Llanvirnian (= Floian–Darriwilian) sequence comprises dark-grey to black shales and siltstones, intercalating in places, with minor limestones

and cherts, c. 100–130 m in thickness (Sobolevskaya, 2011). This contrasts with > 980 m of upper Floian – lower Darriwilian turbidites in Bennett Island. However, both sequences indicate a deep-water origin. During the 2016 expedition, we observed rhythmic packages composed of mudstone-calcsiltite (or calcarenite) intercalation within this interval in the NE part of Central Taimyr zone. The carbonate siltstones demonstrate current ripples; some parts of the section are obviously carbonate turbidites with their characteristic features (Supplementary Figs S29–S31).

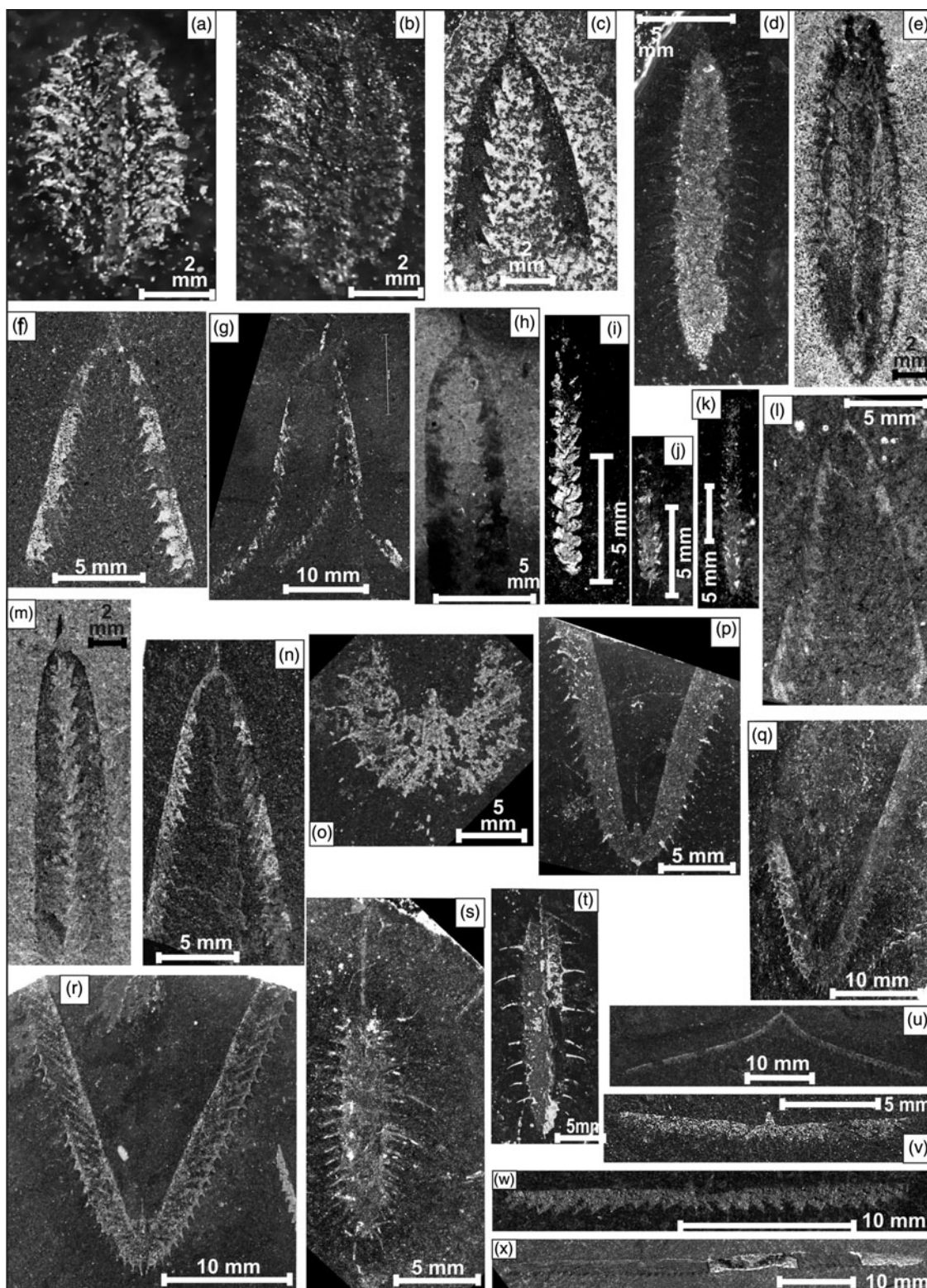


Fig. 29. Ordovician graptolites from Bennett Island. (a, b) *Phyllograptus rotundatus* Mosen, location 226/1. (c) *Dydimograptus* aff. *stabilis* Elles et Wood, location 140/1. (d, s) *Glossograptus hincksi* (Hopkinson), location 138/1. (e) *Pseudophyllograptus angustifolius elongatus* Bulman, location 140/1. (f) *Didymograptus protobifidus* Elles, location 223/3. (g) *Pendeograptus* aff. *fruticosus* (Hall), location 223/1. (h) *Didymograptus* aff. *protobifidus* Elles, location 140/1. (i, j) Transit forms *Undulograptus austrodentatus* (Harris et Keble) – *Undulograptus sinodentatus* (Mu et Lee), location 103/1. (k) *Undulograptus* sp., location 103/1. (l) *Didymograptus protobifidus* Elles, location 283/1. (m) *Didymograptus* ex gr. *indentus* (Hall), location 140/1. (n) *Didymograptus protobifidus* Elles, location 225/2. (o) *Isograptus caduceus nanus* (Ruedemann), location 136/1. (p) *Isograptus* ex gr. *maximo-divergens* (Harris), location 138/1. (q, r) *Isograptus gibberulus* (Nicholson), location 249/1. (t) *Glossograptus acanthus* Elles et Wood, location 108/8b. (u) *Corymbograptus deflexus* (Elles et Wood), location 224/1. (v) *Expansograptus taimyrensis* Obut et Sobolevskaya, location 224/1. (w) *Expansograptus suecicus* (Tullberg), location 225/2. (x) *Expansograptus latus* (Hall), location 224/1.



Fig. 30. Ordovician conodonts from Bennett Island. The collection of conodonts is kept at the AP Karpinsky Russian Geological Research Institute (St Petersburg). (a–d, g) *Oepikodus* cf. *intermedius* (Serpagli), sample 114/2: (a) S element, $\times 72$; (b) Sd element, $\times 86$; (c) P element, $\times 105$; (d) P element, $\times 83$; (g) M element, $\times 61$. (e, f) *Paracordylodus gracilis* Lindström, 1955, sample 114/2: (e) P? element, $\times 107$; (f) S element, $\times 125$. (h, k, l, o) *Acodus* sp., sample 114/2: (h) Sd element, $\times 115$; (k) Sd element, $\times 92$; (l) Sa element, $\times 94$; (o) P element, $\times 102$. (i) *Jumodontus* sp., sample 114/2, $\times 75$. (j, n) *Kallidontus corbatoi* (Serpagli, 1974), sample 114-2: (j) P element, $\times 68$; (n) S element, $\times 73$. (p) *Cornuodus longobasis* (Lindström, 1955), sample 114/2, $\times 79$. (q) *Protopanderodus* sp., sample 114-2, S element, $\times 48$. (r) *Lundodus gladius* (Lindström, 1955), sample 114/2, P element, $\times 64$. (s) *Protoprioniodus papillosus* (van Wamel, 1974), sample 114/2, Sa element, $\times 78$. (t, u) *Paroistodus horridus* (Barnes & Poplawski, 1973), sample 313/1: (t) M? element, $\times 67$; (u) S element, $\times 54$. (v, w) *Periodon* cf. *macrodentata* (Graves & Ellison, 1941), sample 313/1: (v) S element, $\times 54$; (w) M element, $\times 45$.

7.c. Siberian Platform

On the Siberian Platform the Ordovician deposits are observed in outcrops and wells throughout the area except for the northeastern part, where this stratigraphic interval is absent. In the NW zone of the platform (in the region of Noril'sk; Figs 28, 29), the upper Cambrian and Ordovician deposits are represented by shallow-water tropical limestones and dolomites several hundreds of metres thick, including clayey limestones and oolitic grainstones in places (Kanygin et al. 2007, 2010). The upper Floian – lower Darriwilian interval is a variegated unit (100–200 m) that, apart from carbonate rocks, contains a significant volume of siltstones, some evaporites and sandstone layers in its middle part. A similar

but more clayey unit (40 m) forms the very tops of the Darriwilian and the lower Sandbian strata. The total thickness of the Lower–Middle Ordovician deposits here is c. 800 m.

To the NE of the Noril'sk region (Ambardakh River; Figs 28, 29), the uppermost Cambrian–Tremadocian deposits consist mainly of coloured dolomites and clayey dolomites with mudstones and gypsum; the Floian deposits comprise clayey and sandy dolomites and limestones. The Lower Ordovician strata have a thickness of about 250 m and contain layers and lenses of carbonate(?) conglomerates. They are overlain by coastal quartz sandstones of the Dapingian – lower Darriwilian deposits (up to 50 m) on eroded surface, of which the lower Silurian limestones rest. To the NE, the depth of erosion increases rapidly and,

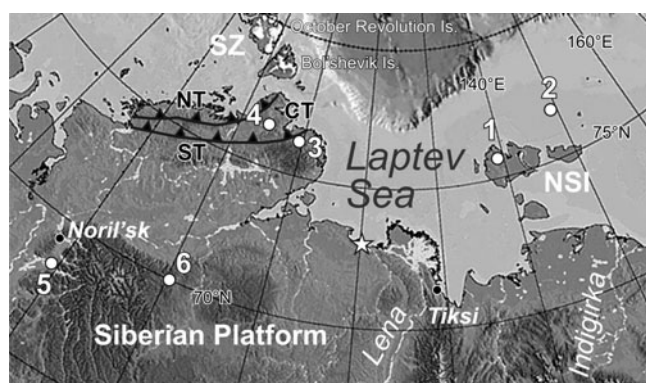


Fig. 31. Location of the Ordovician successions discussed in Sections 6 and 7.a. 1, NE part of Kotel'ny Island; 2, Bennett Island; 3, Southern Taimyr (eastern part); 4, Central Taimyr (eastern part); 5, Siberian platform, Noril'sk area; 6, Siberian platform, Ambardakh River. Asterisk represents Ust'-Olenek borehole position. NSI – New Siberian Islands; SZ – Severnaya Zemlya; ST, CT, NT – Southern, Central and Northern Taimyr zones, respectively.

approximately 80 km to the NE (the middle course of the Maimecha River), the lower Palaeozoic section ends by the top of the Lower Ordovician Series (Kanygin *et al.* 2007; Zhamoïda, 2014). Further to the ENE within the Siberian Platform the Ordovician deposits are absent, but they are known in the Ust'-Olenek borehole at the Laptev Sea coast (Fig. 31). Here the Vendian(?) carbonate rocks are overlain by Middle Ordovician – lower Silurian shallow-marine limestones and dolomites (VV Grausman, unpub. PhD thesis, Siberian Research Institute of Geology, Geophysics and Mineral Resources, 1994).

Thus, within the northern part of the Siberian Platform, the Lower Ordovician deposits show a transition from west to east from an open shelf facies to comparatively nearshore facies (including lagoonal), and the Middle Ordovician deposits show a transition from restricted inner shelf to coastal facies.

In general, the Ordovician deposits in the north of Siberia have much in common with those of Kotel'ny Island. The differences are due to the proximity of the first region to a land. A notable feature of Siberian succession is the Middle Ordovician siliciclastic sandstones, which are thought to be a response to general regression and humidization of the climate (Kanygin *et al.* 2007). In the opinion of AV Dronov, siliciclastic turbidites of Bennett Island provide an analogue of the Middle Ordovician quartz sandstones, widespread in Siberia, and marking the destruction of the warm-water carbonate platform, but in deeper-water facies (AV Dronov, pers. comm., 2017).

7.d. Northern Alaska

Both Ordovician carbonate platform rocks and coeval deep-water turbidites are known in the Seward Peninsula (northern Alaska; Dumoulin *et al.* 2014). Sections under discussion belong to the York terrane (Supplementary Fig. S32). The carbonate rocks build up so-called York successions of mostly shallow to very shallow-water facies (Fig. 32). The lower part of the succession is Tremadocian–Darrivilian in age; the younger part contains Upper Ordovician, Silurian and Devonian(?) strata. Some deep-water incursions took place during late Early Ordovician (Early Floian?) time and then during Middle Ordovician time. Graptolitic black shales occur near the Lower–Middle Ordovician boundary and grade upwards into carbonate turbidites. Relatively shallow settings resumed during latest Middle

Ordovician time. Dumoulin *et al.* (2014) suggested intraplateform basin environments for these shales and turbidites. Another turbidite sequence crops out within the York terrane WNW of the York succession exposures (Supplementary Fig. S32). The lower part of the sequence comprises Neoproterozoic – earliest Cambrian siliciclastic turbidites and could act as a basement for carbonate platform strata. The upper part consists of mixed carbonate-siliciclastic turbidites, interpreted as basinal equivalents of the York succession (Fig. 32). Its Ordovician age is constrained only by single conodont specimen (Dumoulin *et al.* 2014).

The Ordovician rocks in the York succession formed a part of the Cambrian–Devonian Northern Alaska carbonate platform. Its other parts crop out in the east Seward Peninsula (metacarbonates within the Nome Complex), Brooks Range and inland Alaska (Farewell and White Mountains terranes). The Ordovician was the period during which lithological and faunal similarities between these areas and also with Chukotka and 'peri-Siberian terranes' (Kotel'ny, Omulevka) were the strongest (Dumoulin *et al.* 2014). Several authors suggest that the Middle–Upper Ordovician carbonate rocks in NE Chukotka represent a part of this platform, as noted above (see Section 7.a; Oradovskaya & Obut, 1977; Şengör & Natal'in, 1996; Natal'in *et al.* 1999). The Alaskan carbonate platform strata together with coeval turbidites were components of the Neoproterozoic–Devonian passive margin of the Arctic Alaska–Chukotka terrane (excluding the North Slope subterrane; see Strauss *et al.* 2013). This terrane probably originated within a continuation of the Timanide orogen of Baltica and was situated between Laurentia, Siberia and Baltica during the Ordovician Period, with its western part (present-day coordinates) being close to Siberia (Dumoulin *et al.* 2014).

7.e. Northern Taimyr and Severnaya Zemlya

Large parts of the Northern Taimyr Zone and Bol'shevik Island (southern Severnaya Zemlya; Fig. 31) are made of thick metamorphosed flysch-like sequence, which includes upper Neoproterozoic(?), Cambrian and Lower Ordovician sediments (Lorenz *et al.* 2008; Pease & Scott, 2009; Kachurina *et al.* 2012). The unit comprises a rhythmic intercalation of sandstones, siltstones and shales in different proportions; in some intervals rocks are calcareous. Carbonate concretions and minor gritstone occur.

The lower Palaeozoic flysch on Bol'shevik Island is coeval with shallow-marine, predominantly siliciclastic, fossiliferous rocks exposed to the NW on October Revolution Island (Kuz'min *et al.* 2000). This indicates SE-wards deepening of the Cambrian–Ordovician basin (Lorenz *et al.* 2008). It should be noted that on October Revolution Island, Lower Ordovician rocks contain volcanic rocks that were interpreted as rift-related (Kuz'min *et al.* 2000).

According to published data (Lorenz *et al.* 2008; Pease & Scott, 2009; Kachurina *et al.* 2012; Ershova *et al.* 2016), Northern Taimyr flysch shares many similarities with the siliciclastic turbidites of Bennett Island, especially in detrital zircon age distribution, implying they could have the same provenance.

7.f. Ordovician Bennett Basin: Siberian inherency and possible genesis

The Ordovician sedimentary basin, represented in the deposits of Bennett Island, inherited the Cambrian basin that was a continuation of the Siberian Platform (Danukalova *et al.* 2014). This

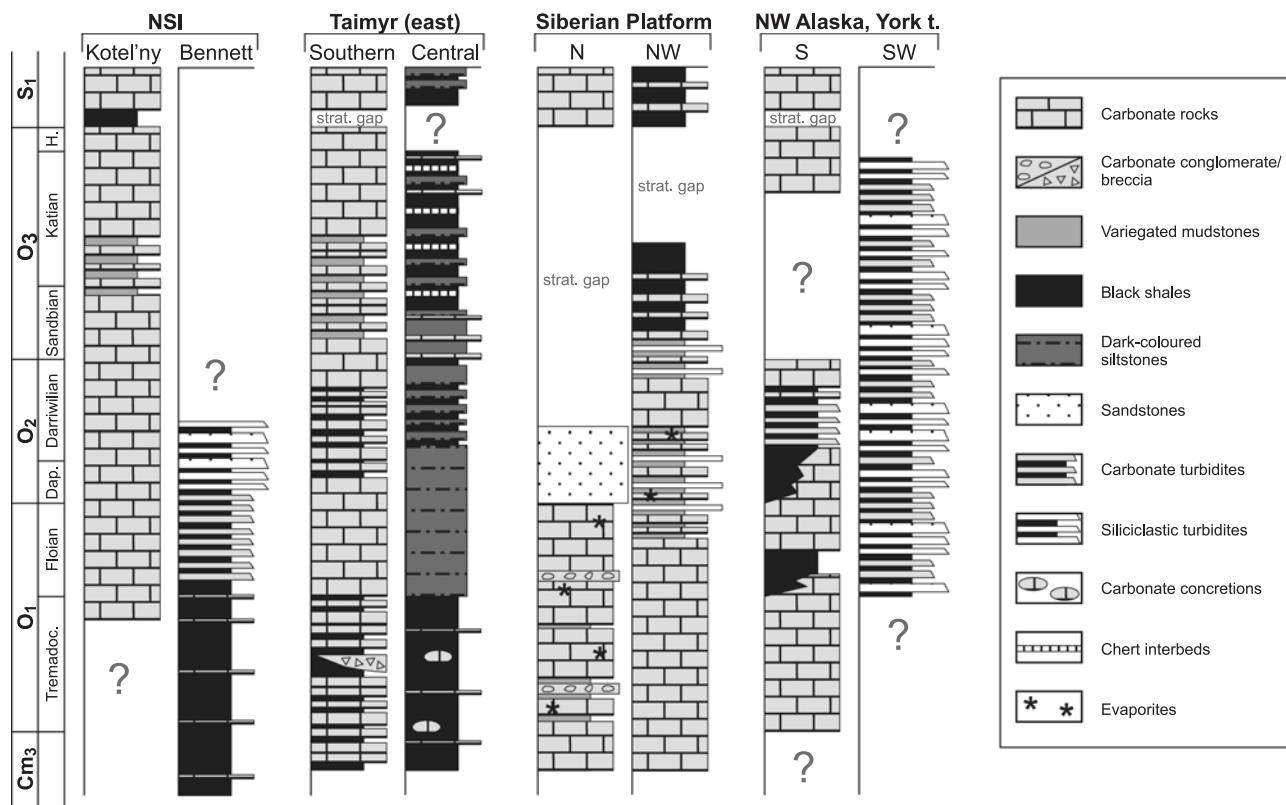


Fig. 32. Correlation of the Ordovician units in the Eastern Arctic (from left to right): New Siberian Islands including NE Kotel'ny Island (Kos'ko *et al.* 1985) and Bennett Island (this paper); eastern part of Taimyr (Southern and Central domains) (Sobolevskaya, 2011; Zhamoïda, 2014); Siberian platform (northern part, Ambardakh River, and NW part, Noril'sk area) (Kanygin *et al.* 2007; Tesakov, 2012; Zhamoïda, 2014); NW Alaska (Seward Peninsula, York terrane: southern part, York succession and SW part, deep-water age equivalents?) (Dumoulin *et al.* 2014). Age of the upper part of turbidite succession in SW York terrane is poorly constrained (based on middle Early – Late Ordovician conodont). For location of sections see Supplementary Figure 31 and Supplementary Fig. S30. NSI – New Siberian Islands; York t. – York terrane; Tremadoc. – Tremadocian; Dap. – Dapingian; H. – Hirnantian; Cm₃ – Upper Cambrian.

conclusion is based on: the similarity of Cambrian trilobite faunas dominated by endemic Siberian species; lithological similarity of some levels of the sequence; and the synchronicity of the geological events, reflected in the lithostratigraphic subdivision of the Cambrian section into coeval units in both territories. Consequently, the Ordovician rocks of Bennett Island were accumulated, or at least began to accumulate, in a deep-water trough that was still within the Siberian palaeocontinent (Fig. 33). It can be assumed that to the south of this trough there was a shallow zone of the basin with prevailing carbonate sedimentation, represented by the Kotel'ny Island and Southern Taimyr successions. Following this logic, we can assume that the continuation of the Bennett trough was located in the Central Taimyr zone. The deposits of these two regions do in fact exhibit many common features, but they also demonstrate significant differences in palaeotectonic interpretation. It is assumed that the Taimyrian sequence accumulated on the passive margin of Siberia, contiguous with the continuation of the Uralian Ocean during Ordovician time (e.g. Vernikovskiy, 1996).

The Bennett basin succession could not mark the Ordovician margin of Siberia palaeocontinent because clastic material was supplied from the opposite side (see Section 5.g), that is, from the same non-volcanic source as during Cambrian time (Danukalova *et al.* 2014; Ershova *et al.* 2016). Based on clastic transport direction and detrital zircon ages (Ershova *et al.* 2016), the Middle Ordovician siliciclastic flysch of Bennett Island could be correlated with equivalent rocks in the Northern Taimyr (see Section 7.e).

This contradiction can be resolved by the assumption that there was no ocean basin between Central and Northern Taimyr domains during early Palaeozoic time, as proposed in Kaban'kov *et al.* (2003) and Lorenz *et al.* (2008).

We therefore suggest that the Bennett basin developed within a vast 'New Siberian – Siberian' carbonate platform as a relatively deep-water trough. The carbonate platform supplied the Ordovician Bennett basin with carbonate debris that dominates in the Middle Unit and occurs in considerable quantities in the Upper Unit. This platform could extend up to Northern Alaska (see Sections 7.1 and 7.4) where, in the York terrane, Ordovician deep-water black shales and carbonate turbidites accumulated in an intraplatform basin(s) (Dumoulin *et al.* 2014). The Bennett basin possibly developed due to rifting.

The Ordovician rifting was reported in different Arctic terranes. Till *et al.* (2014) assume that rift-related mafic magmatism on Seward Peninsula (Arctic Alaska) occurred during Early–Middle Ordovician time. The Early Ordovician rifting and associated magmatism was also proposed on October Revolution Island (Proskurnin, 1995; Kuz'min *et al.* 2000; Lorenz *et al.* 2007, 2008). Rifting events in both regions are thought to be related to the extensional regime during the opening of the Uralian Ocean (Lorenz *et al.* 2008; Pease & Scott, 2009; Till *et al.* 2014). Possible confirmation of the Ordovician rifting can be found in the New Siberian Islands; Ordovician igneous rocks are known of on Henrietta Island (Kaplan *et al.* 2001) and are presumably rift-related (Vinogradov *et al.* 1975; NA Goryachev, pers. comm.,

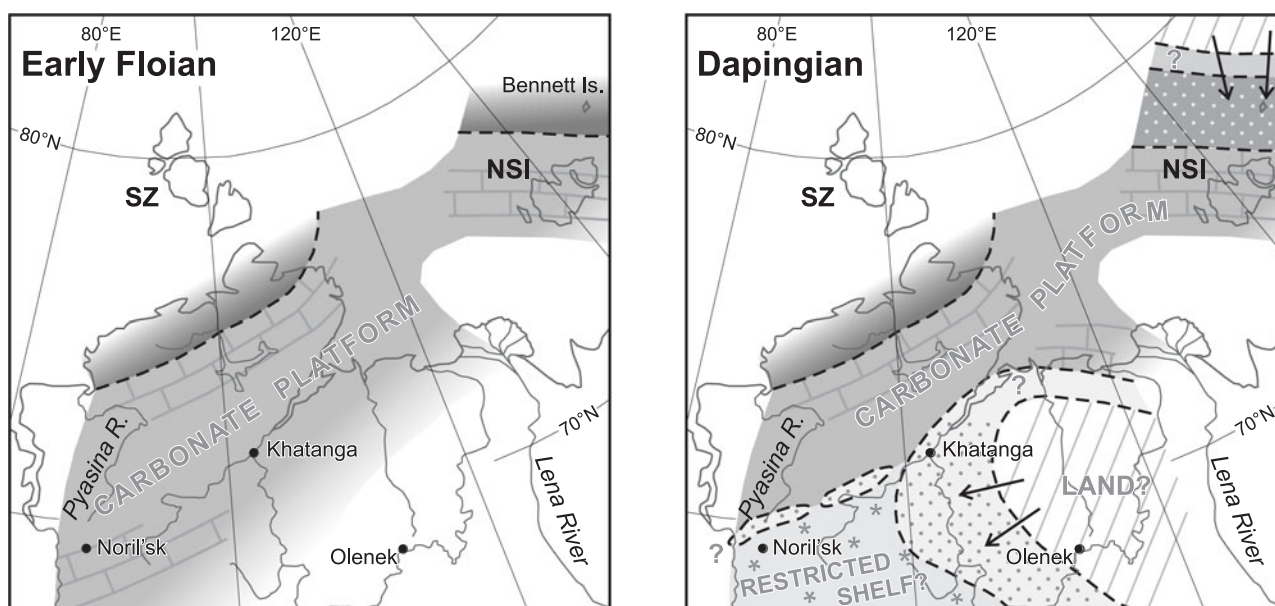


Fig. 33. Proposed palaeogeography for earliest Floian and Dapingian time of northern Siberia, Taimyr and New Siberian Islands (shown on the present-day map). Dotted pattern marks siliciclastic-rich facies; stars represent coloured deposits with evaporites. Distance between Bennett Island and proposed land to the NE is not to scale. SZ – Severnaya Zemlya; NSI – New Siberian Islands. Data on Northern Taimyr and Severnaya Zemlya (Kara block) were not used in the reconstructions. White area in the SE Laptev Sea corresponds to a possible absence of Ordovician deposits.

2015; Kuzmichev & Danukalova, unpublished data). However, other geologists believe that magmatism on Henrietta Island is of the island-arc type (Kos'ko & Korago, 2009; Ershova *et al.* 2016).

8. Conclusions

Study of the Ordovician sequence on Bennett Island revealed three stages in the evolution of the sedimentary basin. At the beginning of Late Cambrian time, the shallow-water Bennett basin started to become deeper and anoxic (Danukalova *et al.* 2014), which led to the deposition of the thick Upper Cambrian – lowermost Ordovician (Tremadocian – Lower Floian) black shale unit (thickness not less than 250 m). The Cambrian–Ordovician boundary position is tentative due to a lack of fossils in the large part of the unit; we propose that 130–140 m of it belongs to the Ordovician System. The deepening of the basin progressed and it was later filled with carbonate turbidites (> 250 m) during Floian – early Dapingian time. Carbonate clastics originated from the nearby carbonate platform. During Dapingian – early Darriwilian time, siliciclastic turbidites were accumulated (thickness not less than 730 m). Mature silicate clastic material (mostly quartz) was transported from remote uplands located to the NE (present-day coordinates). Fragments of shallow-marine fauna came from a carbonate shelf fringing the basin.

We assume that the Bennett basin, part of the Siberian palaeocontinent during Cambrian time, continued to be connected to it during Ordovician time although its counterparts in Siberia became less evident. The Bennett Ordovician basin shared some mutual features with both Central and Northern Taimyr zones. The development of the Bennett turbidite trough in the Ordovician Period was possibly caused by rifting proposed for that time for different Arctic terranes. A similar situation was suggested for northern Alaska (York terrane), where intraplatform turbidite basins were formed within the vast carbonate platform during Early–Middle Ordovician rifting. It is also possible that the

Northern Alaska carbonate platform was connected to the 'Siberian – New Siberian' platform in the Ordovician Period.

Supplementary Material. To view supplementary material for this article, please visit <https://doi.org/10.1017/S0016756819001341>

Acknowledgements. This study has been carried out following the plans of the scientific research of the Geological Institute of RAS (for MKD, ABK, project no. 0135-2015-0020) and was supported by the Russian Foundation for Basic Research (ABK, MKD, grant nos 19-05-00926 and 14-05-31042; NVS, grant no. 18-0570035). We thank Thomas Hadlari and an anonymous reviewer for their helpful comments.

Declaration of Interest. The authors are unaware of any conflicts of interest related to this article.

References

- Amy LA, Talling PJ, Peakall J, Wynn RB and Arzola Thynne RG (2005) Bed geometry used to test recognition criteria of turbidites and (sandy) debrites. *Sedimentary Geology* **179**, 163–74.
- Barnes CR and Poplawski MLS (1973) Lower and Middle Ordovician conodonts from the Mystic Formation, Quebec, Canada. *Journal of Paleontology* **47**, 760–90.
- Bergstrom S, Lofgren A and Maletz J (2004) The GSSP of the Second (Upper) Stage of the Lower Ordovician Series: diabasbrottet at Hunneberg, Province of Vastergotland, Southern Sweden. *Episodes* **27**, 265–72.
- Bezzubtsev VV, Zalyalyaev RSh and Sakovich AB (1986) Geological map of Mountain Taimyr. Scale 1: 500 000. Explanatory note. Krasnoyarsk: Krasnoyarskgeologiya, 177 pp. (in Russian).
- Cherkesova SV (1975) Comparative analysis of Lower-Middle Devonian deposits of western Kotel'ny Is. and other Arctic regions. In *Geology and Mineral Resources of New Siberian Islands and Wrangel Island* (ed. D. A. Vol'nov), pp. 22–77. Leningrad: NIIGA (in Russian).
- Cocks LRM and Torsvik TH (2011) The Palaeozoic geography of Laurentia and western Laurussia: a stable craton with mobile margins. *Earth-Science Reviews* **106**, 1–51.

- Danukalova MK, Kuzmichev AB and Korovnikov IV (2014) The Cambrian of Bennett island (New Siberian Islands). *Stratigraphy and Geological Correlation* **22**, 347–69.
- Danukalova MK, Tolmacheva TYu, Männik P, Suyarkova AA, Kul'kov NP, Kuzmichev AB and Melnikova LM (2015) New data on the stratigraphy of the Ordovician and Silurian of the central region of Koteln'y Island (New Siberian Islands) and correlation with the synchronous successions of the Eastern Arctic. *Stratigraphy and Geological Correlation* **23**, 468–94.
- De Long GW (1883) *The Voyage of the Jeannette. Vol. II.* (ed. E. De Long). Boston: Houghton, Mifflin and Co., 911 pp.
- Drachev SS (2011) Tectonic setting, structure and petroleum geology of the Siberian Arctic offshore sedimentary basins. In *Arctic Petroleum Geology* (eds AM Spencer, AF Embry, DL Gautier, AV Stoupakova and K Sørensen), pp. 369–94. Geological Society of London, Memoir no. 35.
- Dumoulin JA, Harris AG, Gagiev M, Bradley DC and Repetski JE (2002) Lithostratigraphic, conodont, and other faunal links between lower Paleozoic strata in northern and central Alaska and northeastern Russia. In *Tectonic Evolution of the Bering Shelf–Chukchi Sea Arctic Margin and Adjacent Landmasses* (eds EL Miller, A Grantz and SL Klemperer), pp. 291–312. Geological Society of America, Boulder, Special Paper no. 360.
- Dumoulin JA, Harris AG and Repetski JE (2014) Carbonate rocks of the Seward Peninsula, Alaska: their correlation and paleogeographic significance. In *Reconstruction of a Late Proterozoic to Devonian Continental Margin Sequence, Northern Alaska, its Paleogeographic Significance, and Contained Base-Metal Sulfide Deposits* (eds JA Dumoulin and AB Till), pp. 59–110. Geological Society of America, Boulder, Special Paper no. 506.
- Ermolaev MM and Spizharsky TN (1947) The De Long Islands. In *Geology of the USSR. V. XXVI* (ed. T. N. Spizharsky), pp. 366–387. Moscow-Leningrad: Ministry of Geology of the USSR (in Russian).
- Ershova VB, Lorenz H, Prokopiev AV, Sobolev NN, Khudoley AK, Petrov EO, Estrada S, Sergeev S, Larionov A and Thomsen TB (2016) The De Long Islands: a missing link in unraveling the Paleozoic paleogeography of the Arctic. *Gondwana Research* **35**, 305–22.
- Graves RW and Ellison S (1941) Ordovician conodonts of the Marathon Basin, Texas. *University of Missouri, School of Mines and Metallurgy, Technical Series Bulletin* **14**, 1–26.
- Kaban'kov V Ya, Sobolevskaya RF and Proskurnin VF (2003) Late Precambrian – Early Paleozoic history of Novaya Zemlya – Taimyr – Severnaya Zemlya fold-and-thrust system. In *Taimyr's Natural Resources* (ed. ON Simonov), pp. 210–228. Dudinka: Ministry of Natural Resources of the Russian Federation (in Russian).
- Kachurina NV, Makariev AA, Makarieva EM, Gavrish AV, Orlov VV and Dymov VA (2012) *The 1 : 1 000 000 State geological map of Russian Federation. Sheet T-45-48. Cape Chelyuskin. Explanatory note.* St Petersburg: VSEGEI, 472 pp. (in Russian).
- Kanygin A, Dronov A, Timokhin A and Gonta T (2010) Depositional sequences and palaeoceanographic change in the Ordovician of the Siberian craton. *Palaeogeography, Palaeoclimatology, Palaeoecology* **296**, 285–94.
- Kanygin AV, Yadrenkina AG, Timokhin AV, Moskalenko TA and Sychev OV (2007) *Stratigraphy of Oil and Gas Basins of Siberia. The Ordovician of Siberian Platform.* Novosibirsk: Geo, 269 pp. (in Russian).
- Kaplan AA, Coppland P, Bro EG, Korago EA, Proskurnin VF, Vinogradov VA, Vrolijk PJ and Walker JD (2001) New radiometric ages of igneous and metamorphic rocks from the Russian Arctic. In *Abstracts of AAPG Regional Conference, St. Petersburg, 2001*, p. 6. St Petersburg: VNIGRI and AAPG.
- Koren' TN, Tolmacheva TYu, Sobolevskaya RF, Raevskaya EG and Obut OT (2006) *The Ordovician System. Zonal Stratigraphy of the Phanerozoic of Russia.* St Petersburg: VSEGEI, pp. 31–47 (in Russian).
- Kos'ko M and Korago E (2009) Review of geology of the New Siberian Islands between the Laptev and the East Siberian Seas, North East Russia. In *Geology, Geophysics and Tectonics of Northeastern Russia: A Tribute to Leonid Parfenov* (eds DB Stone, K Fujita, PW Layer, EL Miller, AV Prokopiev and J Toro), pp. 45–64. Stephan Mueller Special Publication, Series 4. Published by Copernicus Publications on behalf of the European Geosciences Union.
- Kos'ko MK, Bondarenko NS and Nepomiluev VF (1985) *The 1 : 200000 State Geological Map of the USSR. Sheets T-54-XXXI, XXXII, XXXIII; S-53-IV, V, VI, XI, XII; S-54-VII, VIII, IX, XIII, XIV, XV. Explanatory Note* (ed. VI Ustritskii). Moscow: Ministry of Geology of the USSR, 162 pp. (in Russian).
- Kuz'min VG, Avdunichev VV, Gavrish AV, Lazurkin DV, Proskurnin VF, Smirnov AN, Ushakov VI, Fokin VI and Shulga YuD (2000) Severnaya Zemlya: Geology and minerageny. In *Geology and Minerageny* (eds IS Gramberg and VI Ushakov). St Petersburg: VNIIOkeangeologiya, 187 pp. (in Russian).
- Lindström M (1955) Conodonts from the lowermost Ordovician strata of south-central Sweden. *Geologiska Föreningens i Stockholm Förhandlingar* **76**, 517–604.
- Lofgren A (1994) Arenig (Lower Ordovician) conodonts and biozonation in the Eastern Siljan district, Central Sweden. *Journal of Paleontology* **68**, 1350–68.
- Lorenz H, Gee DG and Simonetti A (2008) Detrital zircon ages and provenance of the Late Neoproterozoic and Palaeozoic successions on Severnaya Zemlya, Kara Shelf: a tie to Baltica. *Norwegian Journal of Geology* **88**, 235–58.
- Lorenz H, Gee DG and Whitehouse MJ (2007) New geochronological data on Palaeozoic igneous activity and deformation in the Severnaya Zemlya Archipelago, Russia, and implications for the development of the Eurasian Arctic margin. *Geological Magazine* **144**, 105–25.
- Lowe DR (1982) Sediment gravity flows: II. Depositional models with special reference to the deposits of high-density turbidity currents. *Journal of Sedimentary Petrology* **52**(1), 279–97.
- Lowe DW and Guy M (2000) Slurry-flow deposits in the Britannia Formation (Lower Cretaceous), North Sea: a new perspective on the turbidity current and debris flow problem. *Sedimentology* **47**, 31–70.
- Loydell DK (2012) Graptolite biozone correlation charts. *Geological Magazine* **149**, 124–32.
- Männik P and Viira V (2012) Ordovician conodont diversity in the northern Baltic. *Estonian Journal of Earth Sciences* **61**, 1–14.
- McClelland HLO, Woodcock NH and Gladstone C (2011) Eye and sheath folds in turbidite convolute lamination: Aberystwyth Grits Group, Wales. *Journal of Structural Geology* **33**, 1140–7.
- Mitchell CE, Xu C, Bergstrom SM, Yuan-Dong Z, Zhi-Hao W, Webby BD and Finney SC (1997) Definition of the global boundary stratotype for the Darriwilian Stage of the Ordovician system. *Episodes* **20**, 158–66.
- Mulder T, Razin P and Faugeres JC (2009) Hummocky cross-stratification-like structures in deep-sea turbidites: upper Cretaceous Basque basins (Western Pyrenees, France). *Sedimentology* **56**, 997–1015.
- Mutti E and Ricci Lucchi F (1978) Turbidites of the northern Apennines: introduction to facies analysis. *International Geology Review* **20**, 125–66.
- Natal'in BA, Amato JM, Toro J and Wright JE (1999) Paleozoic rocks of northern Chukotka Peninsula, Russian Far East: implications for the tectonics of the Arctic region. *Tectonics* **18**, 977–1003.
- Nekhorosheva LV (1977) Ordovician Bryozoa of the Koteln'y Island (New Siberian Islands). In *Precambrian and Paleozoic Stratigraphy and Paleontology of Northern Siberia* (eds VI Bondarev and NP Lazarenko), pp. 72–92. Leningrad: NIIGA (in Russian).
- Nikishin AM, Malyshev NA and Petrov EI (2015) *Geological Structure and History of the Arctic Ocean.* Houten: EAGE Publications (no pagination).
- Obut AM (1964) Hemichordata. In *Basics of Paleontology* (ed. RF Gekker), pp. 279–337. Moscow: Nedra (in Russian).
- Obut AM and Sobolevskaya RF (1964) *Ordovician Graptolites of Taimyr.* Moscow: Nauka, 92 pp. (in Russian).
- Oradovskaya MM and Obut AM (1977) Stratigraphy, correlation, and paleogeography of the Ordovician and Silurian strata in Chukotka Peninsula. In *Ordovician and Silurian Stratigraphy and Fauna of the Chukotka Peninsula* (ed. AM Obut), pp. 4–42. Novosibirsk: Nauka (Proceedings of the Institute of Geology and Geophysics) (in Russian).
- Pease V and Scott RA (2009) Crustal affinities in the Arctic Uralides, northern Russia: significance of detrital zircon ages from Neoproterozoic and Palaeozoic sediments in Novaya Zemlya and Taimyr. *Journal of the Geological Society* **166**, 517–27.
- Pettijohn FJ, Potter PE and Siever R (1987) *Sand and Sandstone.* New York: Springer, 553 pp.
- Pickering KT, Clark JD, Smith RDA, Hiscott RN, Ricci Lucchi F and Kenyon NH (1995) Architectural element analysis of turbidite systems, and selected topical problems for sand-prone deep-water systems. In *Atlas of Deep Water*

- Environments* (eds KT Pickering, RN Hiscott, NH Kenyon, F Ricci Lucchi and RDA Smith), pp. 1–10. Dordrecht: Springer.
- Pohler SML** (1994) Conodont biofacies of Lower to lower Middle Ordovician megaconglomerates, Cow Head Group, western Newfoundland. *Geological Survey of Canada, Bulletin* **459**, 1–71.
- Proskurnin VF** (1995) New volcano-plutonic association in Severnaya Zemlya and special aspects of its metal content. *Bowels of the Taimyr* (ed. AG Samoilov), pp. 93–100. Norilsk: Taimyrgeolcom (in Russian).
- Pyle LJ and Barnes CR** (2002) *Taxonomy, Evolution and Biostratigraphy of Conodonts from the Kechika Formation, Skoki Formation and Road River Group (Upper Cambrian to Lower Silurian), northeastern British Columbia*. Ottawa: NRC Research Press, 227 pp.
- Pyle LJ and Barnes CR** (2003) Conodonts from a platform-to-basin transect, Lower Ordovician to Lower Silurian, Northeastern British Columbia, Canada. *Journal of Paleontology* **77**, 146–71.
- Rasmussen JA** (2001) Conodont biostratigraphy and taxonomy of the Ordovician shelf margin deposits in the Scandinavian Caledonides. *Fossils and Strata* **48**, 1–80.
- Şengör AMC and Natal'in BA** (1996) Paleotectonics of Asia: fragments of a synthesis. In *The Tectonic Evolution of Asia* (eds A Yin and M Harrison), pp. 486–640. New York: Cambridge University Press.
- Sennikov NV** (1996) *Paleozoic graptolites of Middle Siberia. Systematics, phylogeny, biology, paleozoogeography*. Novosibirsk: SB RAS, 225 pp. (in Russian).
- Sennikov NV** (1998) New graptolite taxa from the Middle Cambrian to Ordovician of Central Siberia. *News of Paleontology and Stratigraphy* **1**, 15–31 (in Russian).
- Serpagli E** (1974) Lower Ordovician conodonts from Precordilleran Argentina (province of San Juan). *Bolletino della Società Paleontologica Italiana* **13**, 17–98.
- Serra F, Albanesi GL, Ortega G and Bergstrom SM** (2015) Biostratigraphy and palaeoecology of Middle–Late Ordovician conodont and graptolite faunas of the Las Chacritas River section, Precordillera of San Juan, Argentina. *Geological Magazine* **152**, 813–29.
- Shanmugam G** (2012) *New Perspectives on Deep-water Sandstones: Origin, Recognition, Initiation, and Reservoir Quality*. Amsterdam: Elsevier, 488 pp.
- Soh W** (1989) Coarse clast dominant submarine debrite, the Mio-Pliocene Fujukawa Group, Central Japan. In *Sedimentary Facies in the Active Plate Margin* (eds A Taira and F Mazuda), pp. 495–510. Tokyo: Terra Scientific Publishing.
- Sobolevskaya RF** (1969) New Late Ordovician graptolites of the Omulevka mountains. *Paleontological Journal* **2**, 9–11 (in Russian).
- Sobolevskaya RF** (1971) New Ordovician graptolites of the Omulevka mountains. *Paleontological Journal* **1**, 82–7 (in Russian).
- Sobolevskaya RF** (1973) On the age of Krivun Formation (Ordovician of the Omulevka mountains). In *New in Paleontology of Siberia and Middle Asia* (ed. AB Ivanovsky), pp. 19–29. Novosibirsk: Nauka (in Russian).
- Sobolevskaya RF** (1974) New Ashgillian graptolites from Kolyma River middle reaches. In *Graptolites of the USSR* (ed. AM Obut), pp. 63–71. Novosibirsk: Nauka (in Russian).
- Sobolevskaya RF** (1976) On Ordovician and Silurian graptolites in New Siberian Islands. In *Graptolites and Stratigraphy* (eds DL Kalio and TN Koren'), pp. 202–9. Tallinn: Estonian SSR Academy of Sciences (in Russian).
- Sobolevskaya RF** (2011) *Atlas of the Paleozoic fauna of Taimyr. Part II. Ordovician and Silurian graptolites*. In *Proceedings of NIIGA-VNIOkeangeologia* **221**. St Petersburg: VNIOkeangeologiya, 282 pp. (in Russian).
- Sorokov DS, Vol'nov DA and Voitsekhovskiy VN** (1961) *The 1:1000000 State Geological Map of the USSR. Sheet S/T-53, 54, 55, 56. Explanatory Note*. Moscow: Gosgeoltechizdat, 60 pp. (in Russian).
- Stouge S** (1982) Preliminary conodont biostratigraphy and correlation of Lower to Middle Ordovician carbonates of the St. George Group, Great Northern Peninsula, Newfoundland. *Newfoundland Department of Mines and Energy, Mineral Development Division, Report* **82**, 1–59.
- Stow DAV** (2012) *Sedimentary Rocks in the Field: A Color Guide*. New York: Academic Press, 320 pp.
- Strauss JV, Macdonald FA, Taylor JF, Repetski JE and McClelland WC** (2013) Laurentian origin for the North Slope of Alaska: implications for the tectonic evolution of the Arctic. *Lithosphere* **5**(5), 477–82.
- Talling PJ, Amy LA, Wynn RB, Peakall J and Robinson M** (2004) Beds comprising debrite sandwiched within co-genetic turbidite: origin and widespread occurrence in distal depositional environments. *Sedimentology* **51**, 163–94.
- Tesakov, Yul** (2012) *Silurian East-Siberian Basin. V. 1. Basin Chronostratigraphy*. Novosibirsk: IPGG SB RAS, 448 pp. (in Russian).
- Till AB, Dumoulin JA, Ayuso RA, Aleinikoff JN, Amato JM, Slack JF and Shanks WCP** (2014) Reconstruction of an early Paleozoic continental margin based on the nature of protoliths in the Nome Complex, Seward Peninsula, Alaska. In *Reconstruction of a Late Proterozoic to Devonian Continental Margin Sequence, Northern Alaska, its Paleogeographic Significance, and Contained Base-Metal Sulfide Deposits* (eds JA Dumoulin and AB Till), pp. 1–28. Geological Society of America, Boulder, Special Paper no. 506.
- Tinterri R, Muzzi Magalhaes P and Tagliaferri A** (2012) Foredeep turbidites of the Miocene Marnoso-arenacea Formation (Northern Apennines). In *Periodico semestrale del Servizio Geologico d'Italia – ISPRA e della Società Geologica Italiana. Geological Field Trips* **4**(2.1), 133 pp. doi: [10.33011/GFT.2012.03](https://doi.org/10.33011/GFT.2012.03).
- Toll' EV** (1904) A brief report to President of the Imperial Academy of Sciences. *Imperial Academy of Sciences Bulletin* **XX**, 158–160 (in Russian and German).
- Tolmacheva TYu** (2014) *Biostratigraphy and Biogeography of the Ordovician Conodonts of the Western Part of Central Asian Orogenic Belt*. St Petersburg: VSEGEI Publishing House, Transactions of VSEGEI, New series **356**, 264 pp.
- van Wamel WA** (1974) Conodont biostratigraphy of the Upper Cambrian and Lower Ordovician of north-western Öland, south-eastern Sweden. *Utrecht Micropaleontological Bulletin* **10**, 1–126.
- Vernikovskiy VA** (1996) *Geodynamic Evolution of Taimyr Folded Area*. Novosibirsk: SPC UIGGM, 202 pp. (in Russian).
- Vernikovskiy VA, Metelkin DV, Matushkin NYu, Tolmacheva TYu, Petrov OV, Sobolev NN and Malyshev NA** (2013) Concerning the issue of paleotectonic reconstructions in the Arctic and of the tectonic unity of the New Siberian Islands Terrane: new paleomagnetic and paleontological data. *Doklady Earth Sciences* **451**, 791–7.
- Vinogradov VA, Kameneva GI and Yavshits GP** (1975) On Hyperborean platform in the light of new data on Henrietta Island geology. In *Arctic Tectonics* (ed. DA Vol'nov), pp. 21–25. Leningrad: NIIGA (in Russian).
- Vol'nov DA and Sorokov DS** (1961) The geology of the Bennett Island. In *Collection of Research Papers on the Geology and Oil and Gas Resources of the Arctic* (ed. BV Tkachenko), pp. 5–18. Leningrad: Gostoptekhizdat, Proceedings of NIIGA **123** (in Russian).
- Vol'nov DA, Voitsekhovskiy VN, Ivanov OA, Sorokov DS and Yashin DS** (1970) New Siberian Islands. In *Geology of the USSR. V. XXVI* (eds BV Tkachenko and BKh Egiazarov), pp. 324–374. Moscow: Nedra (in Russian).
- Wang H, Stouge S, Erdtmann B-D, Chen X, Li Z, Wang C, Zeng Q, Zhou Z and Chen H** (2005) A proposed GSSP for the base of the Middle Ordovician Series: the Huanghuachang section, Yichang, China. *Episodes* **28**, 105–17.
- Webby B, Cooper R, Bergstrom SM and Paris F** (2004) Stratigraphic Framework and Time Scales. In *The Great Ordovician Biodiversification Event* (eds B Webby, F Paris, ML Droser and IG Percival), pp. 41–7. New York: Columbia University Press.
- Wu R, Stouge S, Li Z and Wang Z** (2010) Lower and Middle Ordovician conodont diversity of the Yichang Region, Hubei Province, Central China. *Bulletin of Geosciences* **85**, 631–44.
- Zalasiewicz JA, Taylor I, Rushton AWA, Loydell DK, Rickards RB and Williams M** (2009) Graptolites in British Stratigraphy. *Geological Magazine* **146**, 785–850.
- Zhamoida AI** (ed.) (2014) *Resolutions of the Interdepartmental Stratigraphic Committee on Regional Stratigraphic Schemes of the Siberian Platform, Taimyr, and Altai-Sayan Area*. St Petersburg: VSEGEI, pp. 9–11 (in Russian).